



In silico docking and ADME study of deketene curcumin derivatives (DKC) as an aromatase inhibitor or antagonist to the estrogen-alpha positive receptor ($E\alpha^+$): potent application of breast cancer

Vraj Shah¹ · Jaydip Bhaliya¹ · Gautam M. Patel²

Received: 19 October 2021 / Accepted: 13 December 2021 / Published online: 28 January 2022
© The Author(s), under exclusive licence to Springer Science+Business Media, LLC, part of Springer Nature 2021

Abstract

Regardless of many extensive studies, hormonal-based breast cancer is the most common cause of cancer-related mortality of females worldwide. Indeed, estrogen receptor-positive (ER+) is the communal subtype in breast cancer. To treat this, three types of medications are typically used: selective estrogen receptor modulators (SERMs), selective estrogen receptor down modulators (SERDMs), and aromatase inhibitors (AIs), all of which directly interact with the activation of the estrogen signaling pathway and its formation. Despite their effectiveness, the development of new treatments is required since clinical efficacy is restricted owing to resistance. As a result, in silico studies for drug discovery are booming over the decades because of their affordability and less time-consuming features. Here, 25 deketene curcumin derivatives have been selected for docking studies through MVD software over the positive type of breast cancer through both the treatment hosts $E\alpha^+$ receptor and aromatase. DKC compounds are used because they have several pharmacological uses, including anti-cancer, anti-diabetic, anti-viral, anti-fungal, and anti-bacterial properties. Moreover, an ADME study was carried out for DKC derivatives that reveal the optimum drug-likeness profile. From 25 derivatives, the results showed a better MolDock score, hydrogen bonding, and steric interaction between compounds DKC-10, DKC-20, and DKC-21 with $E\alpha^+$ and aromatase. Although the study was done on both the treatable path hosts, better results were obtained with $E\alpha^+$ as an antagonist. Therefore, it is proposed that three selected DKC derivatives would be better therapeutic agents against breast cancer.

Keywords Estrogen receptor ($E\alpha^+$) · Aromatase · Deketene curcumin · Molegro Virtual Docker (MVD) · Pharmacokinetics

Introduction

Breast cancer is one of the most frequent malignancies in women, with approximately globally 1.7 million new cases being diagnosed each year, with more than 0.5 million deaths [1]. In 2012, 1.67 million instances have been diagnosed, and approximately 522,000 deaths had been reported [2, 3]. In the year 2018, breast cancer led to the

deaths of 627,000 women, accounting for about 15% of all cancer deaths within females. Whereas rates of breast cancer are greater among females in more advanced nations, they are rising in nearly every region around the world. Impacting 2.1 million deaths among women, this information was obtained from the World Health Organization (WHO) [4]. After this, WHO updated the new data on breast cancer cases in the year 2020, according to that 685,000 women deaths due to breast cancer and 2.3 million cases were diagnosed [4a]. Apart from this, breast cancer is on the top list as compared to other cancer types represented in Fig. 1 [4b].

Nowadays, patients with estrogen-dependent breast cancer (EDBC) or hormonal-dependent breast cancer (HDBC) [5] are treated primarily based on a constellation of medical and histopathological criteria, as well as the assessment of three hormonal receptors (HER2 (human epidermal

✉ Gautam M. Patel
gautampatel1573@yahoo.co.in

¹ Department of Chemistry, School of Science, ITM SLS Baroda University, Vadodara 391510, India

² Department of Industrial Chemistry, Institute of Science & Technology for Advanced Studies & Research (ISTAR), CVM University, V.V., Nagar 388120, GJ, India

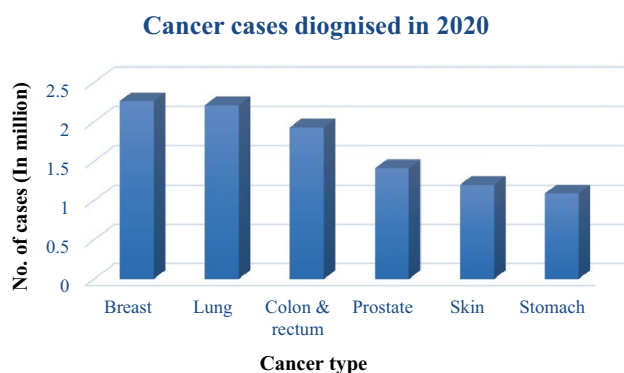


Fig. 1 Diagnosed cases among different cancer types

growth factor receptor 2), estrogen receptor (ER), and progesterone receptor (PR)). Patients with breast cancer who have ER-positive tumors typically have a better prognosis than those who have ER-negative tumors [6]. Additionally, upon reviewing the literature, we discovered that approximately 70 to 75% of breast cancers express positive estrogen receptors (ER α), and the responsible receptors are ER α -positive (ER α^+) [7–10], whereas only 24.9% of breast cancer express the negative estrogen receptor and are considered ER-negative (ER $-$); due to this reason, we have selected ER α -positive as a protein for molecular docking study [8].

Additionally, EDBC-based breast cancer is dependent on estrogen. The aromatization of the A ring results in the production of estrogens, which is catalyzed by the cytochrome p450 enzyme or aromatase; this aromatase is encoded by the CYP19A1 gene [11]. Aromatase converts testosterone (T) and androstenedione (ASD) and then synthesizes estrogens such as estrone (E1) and estradiol (E2) [11–13]. The synthesized estrogens then react with Era, which is encoded by the ESR1 gene that is responsible for breast epithelial cell proliferation and tumor development in cancer patients [14]. Additionally, two pathways exist for suppressing the progression of breast cancer: the first is AIs, which inhibit estrogen production and eventually treat the cancer [15], and the second is antagonist modulators, such as SERDs (selective estrogen down-regulators) and SERMs (selective estrogen receptor modulators), which directly inhibit genomic estrogen signaling [16]. Perhaps AIs are only effective against postmenopausal breast cancer, whereas antagonist modulators are effective against both types of breast cancer [17, 18].

Several medications are available in the drug market for both ways, AIs and antagonists. First is exemestane (AIs) (Fig. 2a). This medicine is used to treat a positive type of breast cancer, and this was approved by US

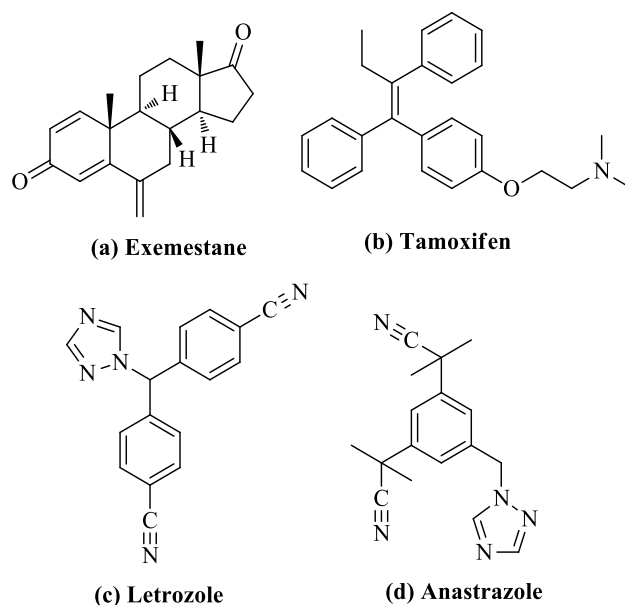


Fig. 2 Chemical structure of drugs used to treat breast cancer. (a) Exemestane, (b) tamoxifen, (c) letrozole, and (d) anastrozole

FDA in the year 2005; this drug is the type of steroidal aromatase inhibitor [19, 20]. Moreover, drug's docking study was done by Setti et al., and that study reveals the MolDock score of -143.607 kcal/mol [21]. Apart from this, another two drugs are utilized to treat the same, which are tamoxifen (Fig. 2b) (antagonist-SERM) under the brand name (like Nolvadex and Soltamox) [22] and letrozole (non-steroidal). Tamoxifen is a widely sold drug but there are certain detrimental drawbacks such as it produces endometrial cancer, blood clot in the lung and legs, stroke, and cataracts. Similarly, letrozole (AIs) (Fig. 2c) consists of hazardous side effects of polycystic ovary syndrome (PCOS) [23, 24]. The docking analysis of these two medicines was carried out by TilakVijay et al. and Verma et al., on breast cancer, which depicted binding affinity of -149.856 and -136.784 kcal/mol, respectively [24, 25]. Another medication on the list is the anastrozole (AIs) (Fig. 2d); this is also a non-steroidal drug that comprises adverse effects such as hot flashes, weakness, bone, joint, and muscle pain or stiffness, sore throat or cough, and high blood pressure [26]. This drug docking investigation was done by Setti et al. and reveals the energy score of -149.521 kcal/mol. Docking data for these medications on breast cancer were obtained using MVD software [21]. On the other hand, some natural products or phytochemicals have been docked for the same disease. For example, Rahman et al. and Thareja et al. used

Table 1 MolDock scores of previously reported drugs against breast cancer by MVD

Sr. no.	Reported ligands	MolDock score (Kcal/mol)	Reference
1	Tamoxifen	-149.856	[25]
2	Anastrozole	-149.521	[26]
3	Exemestane	-143.607	[21]
4	Letrozole	-136.784	[26]

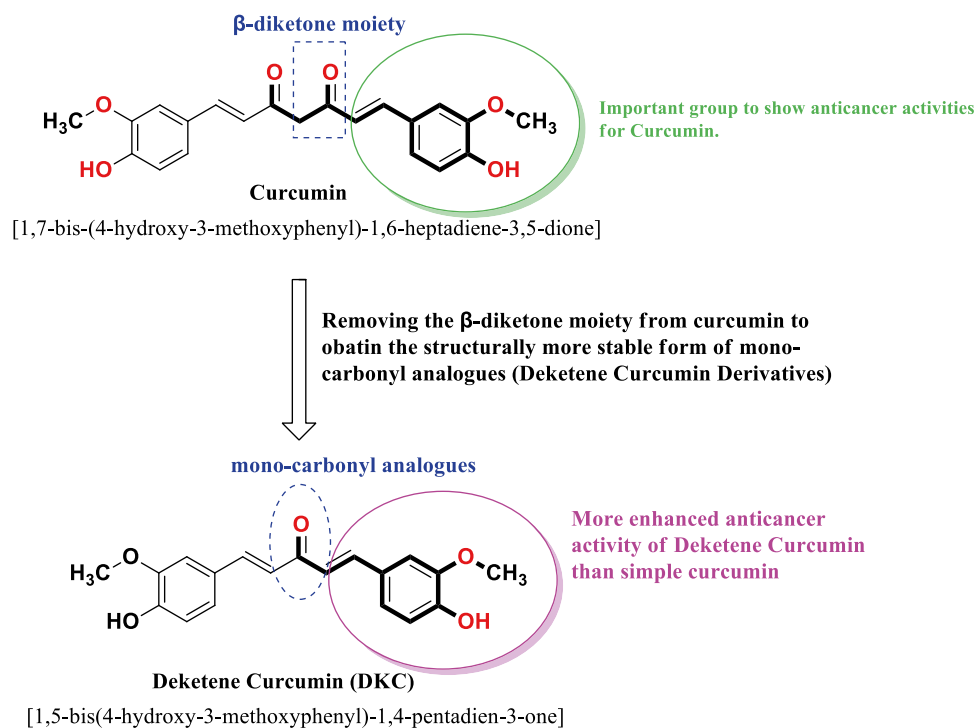
compounds such as abruquiones and flavonoids, which have MolDock scores of -86.309 and -94.36 kcal/mol, respectively [27, 28]. Additionally, these studies' minimum binding affinity values are relatively low in comparison to ours. Table 1.

The purpose of this paper is to identify DKC derivatives with anti-aromatase and anti-Era + receptor activity for use in breast cancer treatment. Indeed, curcumin, a potential anti-cancer agent, has been demonstrated to be more effective in the prevention and treatment of several cancers. Curcumin is a type of polyphenol compound derived from the South Asian plant *Curcuma domestica*. Curcuminoids found in *C. longa* include curcumin, bisdemethoxycurcumin, and demethoxycurcumin. Curcumin is widely used in Ayurveda drugs for a variety of medicinal purposes due to its antioxidant, antiseptic, analgesic, antimalarial, and anti-inflammatory properties.

Curcumin effectively suppresses human carcinomas such as malignant melanoma, cancers of the neck and head, breast, colon, pancreas, prostate, and gonads. Additionally, curcumin derivatives exhibit biological activity against the deadly virus COVID-19 [29]. The inhibitory effects of curcumin compounds on human malignancies are mediated primarily through the control of biochemical cascades, numerous transcription factors, growth factors, pro-inflammatory cytokines, super molecular kinases, and various enzymes [30].

Curcumin's bioavailability, on the other hand, is low due to insufficient stomach absorption, restricted tissue distribution, rapid metabolism, and consequent removal from the body [31]. To address this issue, we chose derivatives of deketene curcumin for a variety of reasons, including the possibility of increasing metabolic stability by omitting the β -diketone moiety (Fig. 3). Despite this, some researchers argue that the presence of the β -diketone moiety is necessary for curcumin's therapeutic properties. Recent research from a variety of agencies confirmed that certain curcumin analogues with a 5-carbon enone spacer but no β -diketone retained or enhanced growth-suppressive activity against various cancer cells. Certain mono-carbonyl analogues of curcumin that lack the β -diketone moiety have been shown greater anti-bacterial and anti-inflammatory activity than curcumin [32]. Compounds with the chemical formula 1, 5-diaryl-1, 4-pentadien-3-ones are the derivatives of

Fig. 3 Structural modification in deketene curcumin, in comparison with curcumin and active sites of the compound responsible for anti-cancer activity [31]



deketene curcumin or mono-carbonyl analogues of curcumin. These are structural analogues of curcumin (1, 7-bis-(4-hydroxy-3-methoxyphenyl)-1, 6-heptadiene-3, 5-Dione), a prominent pigment found in the Indian spice turmeric *Curcuma longa*, Zingiberaceae. The structures of curcumin and deketene curcumin (DKC) are more or less same; however, DKC has greater biological activity than pure curcumin [33].

Certain deketene curcumin derivatives are synthesized and evaluated for their efficacy as anti-cancer agents. In comparison, the technique used to determine whether these compounds can inhibit cancer cell progression is time-consuming and expensive, such as in vivo and in vitro studies. As a result, numerous studies have demonstrated that computational approaches, such as structural bioinformatics and pharmacophore modeling, are the optimal choice due to their high accuracy and reduced time requirements [34]. Docking multiple ligands to the active protein and scoring them to determine binding affinity and interaction intensity has become a widely used technique for virtual screening of large databases as well as lead optimization [35]. On the other hand, the characteristics of a medication's absorption, distribution, metabolism, and elimination (ADME) are critical for a treatment candidate's eventual clinical success. They play a critical role in lowering the failure rate of drug candidates in early-stage clinical trials [36]. Additionally, the synthesis of curcumin derivatives is both environmentally and economically sustainable, as a variety of green routes are available. Numerous benefits can be demonstrated, ranging from high yields to secure, low-cost, and straightforward workup procedures [37].

The present work describes the screening of various deketene curcumin derivatives for their ability to bind directly or indirectly to the ER α -positive receptor and the aromatase enzyme, both of which were obtained from the Protein Data Bank, using the Molegro Virtual Docker software. Apart from this, we conducted ADME studies on the ligands and docking score comparisons with existing drugs used to treat positive type breast cancer. While deketene curcumin derivatives demonstrate potential for both target proteins, they are more effective in terms of binding affinity on the Era + receptor. As a result, DKCs are considered to be effective agents for the treatment of breast cancer.

Computational methodology

Protein and ligand preparation

The crystal structures of ER α + receptor and aromatase which consist of the PDB ID: 3ERT and 3S79 respectively

were directly downloaded from the workspace of software MVD v.7.0.0, where the key of the PDB ID (Protein Data Bank) needs to enter which might be accessed at the URL (<http://www.rcsb.org/pdb>). These IDs have resolutions of 1.90 Å and 2.75 Å correspondingly. Additionally, the downloaded protein contains some ruffled amino acids that are repaired and rebuilt using the mutated and optimization using MVD [38, 39]. The two-dimensional (2D) structures of deketene curcumin derivatives as ligands were obtained using the Chem Bio Draw 12.0.02 computer program. Then, 2D to three-dimensional (3D) representations were converted by the use of Chem Bio 3D 12.0.02 software, and afterward, these were energetically minimized by using a method implemented in the same software and saved as SDF format (*.sdf). Table 2 displays the 2D and 3D structures of all ligands with their specific pharmacological activities. To generate accurate predictions, the imported structures must be properly prepared, which means they must have the correct atom connectivity and bond ordering. This is because when the PDB file is downloaded in its original state, it contains co-factors and water molecules that may cause an error. To address this issue, water molecules and co-factors were manually removed from the MVD after the PDBs were introduced. The absent charges, protonation states, and polar hydrogen allocation were also carried out using a special Molegro algorithm [40].

Cavity or active site detection

Cavity detection is a critical operation that takes place during the docking process. Through the use of a preparation window in the MVD software, efficient binding sites for the selected aromatase and ER α + were identified during this process. This was accomplished through the use of a program called the grid-based anticipation algorithm. Moreover, for the accomplishment of this computational algorithm, the steps had been selected as the greatest numbers of cavities were 5 within 30 × 30 × 30 Å³ cube and the volume was selected between 5 and 10,000 Å. Here, from the five selected cavities, the one with having an optimum value of the cavity has been taken for further consideration in the docking process, such as for aromatase and ER α + the volume (96.256, 364.032 Å³), and surface area (204.8, 844.8 Å²) respectively. Table 3 and Fig. 4a, b illustrate all detected cavities and their associated values such as volume, surface area, and coordinates.

Molecular docking

During the molecular docking process, the energy-optimized conformers of the generated compounds

Table 2 List of deketene curcumin and its derivatives utilized for docking study with aromatase and $\text{Er}\alpha^+$

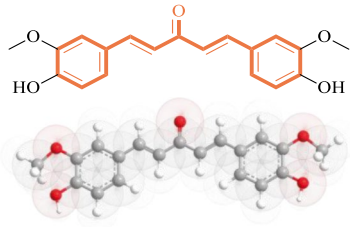
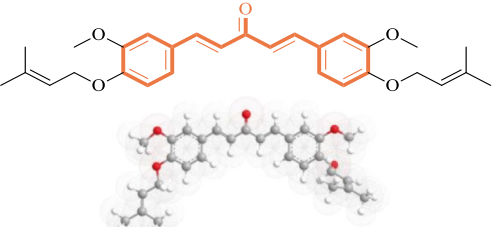
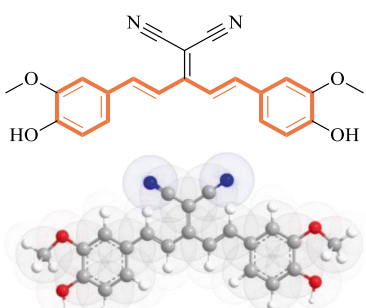
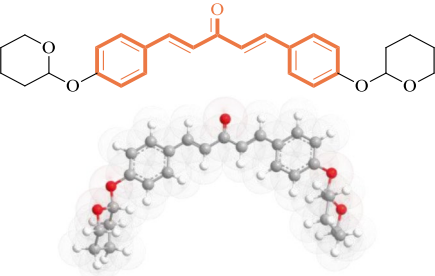
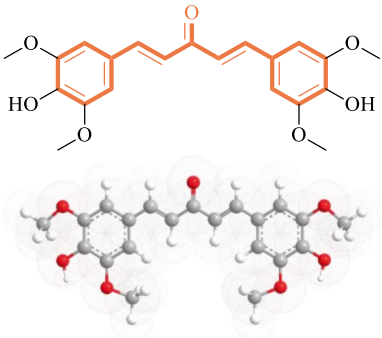
Ligand no	Compound	2D Structure and 3D Structure	Active against	Reference
DKC-1	1,5-bis(4-hydroxy-3-methoxyphenyl)-1,4-pentadiene-3-one		B78H1 melanoma Cells, human colorectal carcinoma cells	[31, 41]
DKC-2	1,5-bis(4-hydroxy-3-methoxyphenyl) pent-1,4-dien-3-ylidenmalononitrile		human tumor cell lines as lung carcinoma NCI-460, melanoma UACC-62, breast MCF-7, colon HT-29, renal 786-O, ovarian OVCAR-03 and ovarian expressing	[33]
DKC-3	1,5-bis(4-hydroxy-3-methoxyphenyl) pent-1,4-dien-3-ylidenmalononitrile		human tumor cell lines as lung carcinoma NCI-460, melanoma UACC-62, breast MCF-7, colon HT-29, renal 786-O, ovarian OVCAR-03 and ovarian expressing	[32]
DKC-4	(1E,4E)-1,5-bis(4-((tetrahydro-2H-pyran-2-yl)oxy)phenyl)pent-1,4-dien-3-one		Active against HL-60 cell line	[32]
DKC-5	(1E,4E)-1,5-bis(4-hydroxy-3,5-dimethoxyphenyl) pent-1,4-dien-3-one		human colorectal cancer cell lines, Antioxidant	[31, 42]

Table 2 (continued)

Ligand no	Compound	2D Structure and 3D Structure	Active against	Reference
DKC-6	((1E,4E)-3-oxopenta-1,4-diene-1,5-diyl)bis(2-methoxy-4,1-phenylene) bis(sulfamate)		growth inhibitory activities on both prostate and breast cancer lines	[43]
DKC-7	((1E,4E)-3-oxopenta-1,4-diene-1,5-diyl) bis(2,6-dimethoxy-4,1-phenylene) bis(sulfamate)		growth inhibitory activities on both prostate and breast cancer lines	[43]
DKC-8	((1E,4E)-1,5-bis(3,5-bis(methoxymethoxy)phenyl)penta-1,4-dien-3-one)		Cell growth inhibition against HCT116	[44]
DKC-9	((1E,4E)-1,5-bis(4-hydroxy-3-methoxyphenyl)penta-1,4-dien-3-one)		inhibit the HIV-1 IN in enzyme assays, Antioxidant	[42, 45]

Table 2 (continued)

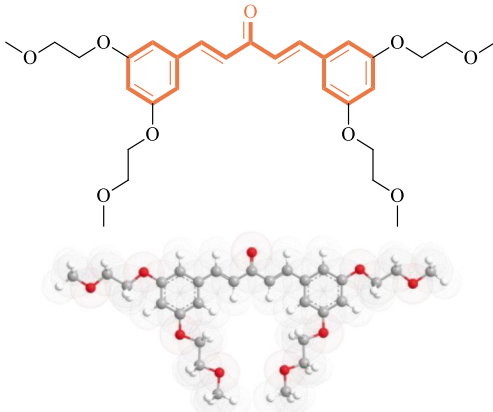
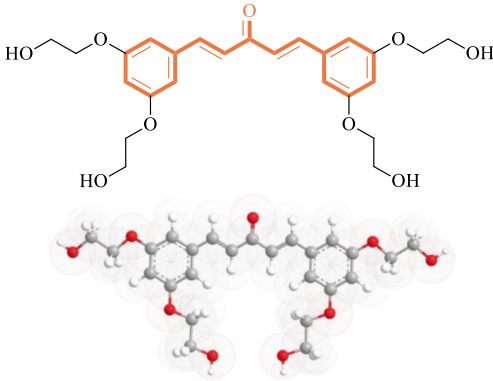
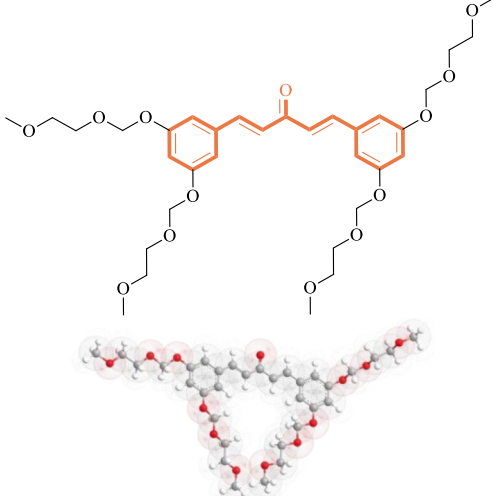
Ligand no	Compound	2D Structure and 3D Structure	Active against	Reference
DKC-11	(1E,4E)-1,5-bis(3,5-bis(2-methoxyethoxy)phenyl)penta-1,4-dien-3-one		Cell growth inhibition against HCT116	[44]
DKC-12	(1E,4E)-1,5-bis(3,5-bis(2-hydroxyethoxy)phenyl)penta-1,4-dien-3-one		Cell growth inhibition against HCT116	[44]
DKC-13	(1E,4E)-1,5-bis(3,5-bis((2-methoxyethoxy)methoxy)phenyl)penta-1,4-dien-3-one		Cell growth inhibition against HCT116	[44]

Table 2 (continued)

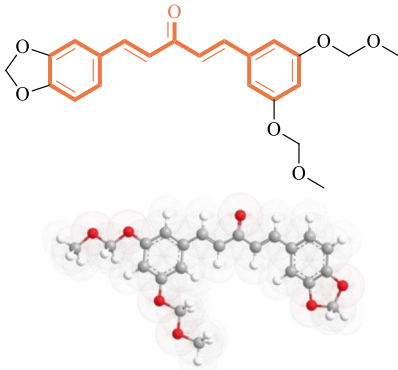
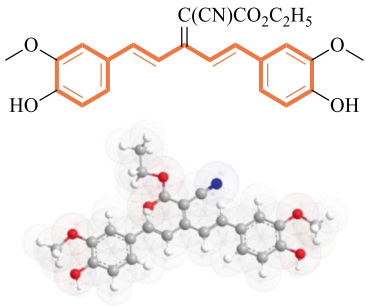
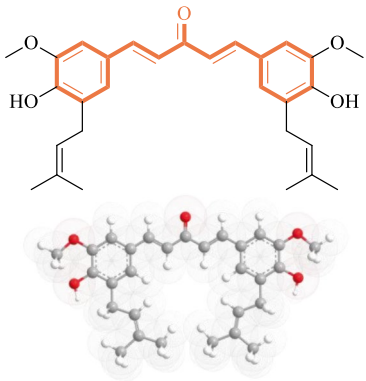
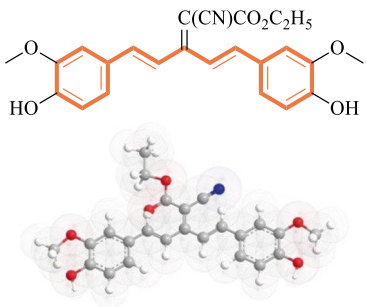
Ligand no	Compound	2D Structure and 3D Structure	Active against	Reference
DKC-14	(1E,4E)-1-(Benzo[d][1,3]dioxol-5-yl)-5-(3,5-bis(methoxymethoxy)phenyl)penta-1,4-dien-3-one		Cell growth inhibition against HCT116	[44]
DKC-15	(E)-ethyl 2-cyano-5-(4-hydroxy-3-methoxyphenyl)-3-((E)-4-hydroxy-3-methoxystyryl)penta-2,4-dienoate		Lung tumor, Melanoma, Normal mamma tumor, (Mamma tumor which expresses the phenotype resistance against multiple drugs), Colon tumor, Renal tumor, Ovary tumor, Prostate tumor, Leukemia	[46]
DKC-16	(1E,4E)-1,5-bis(4-hydroxy-3-methoxy-5-(3-methylbut-2-en-1-yl)phenyl)penta-1,4-dien-3-one		Against various tumor: Lung tumor, Melanoma, Normal mamma tumor, Colon tumor, Renal tumor, Ovary tumor, Prostate tumor, Leukemia	[46]
DKC-17	(E)-ethyl 2-cyano-5-(4-hydroxy-3-methoxyphenyl)-3-((E)-4-hydroxy-3-methoxystyryl)penta-2,4-dienoate		Against various tumor: Lung tumor, Melanoma, Normal mamma tumor, Colon tumor, Renal tumor, Ovary tumor, Prostate tumor, Leukemia	[46]

Table 2 (continued)

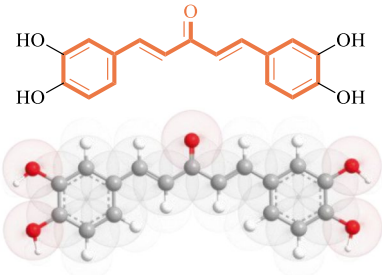
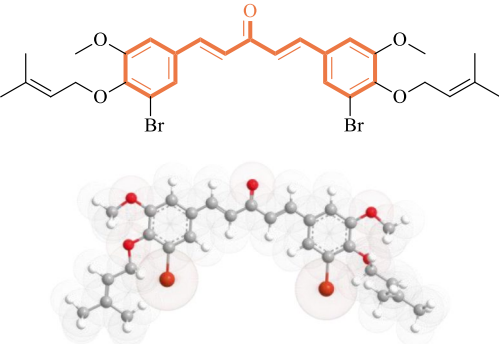
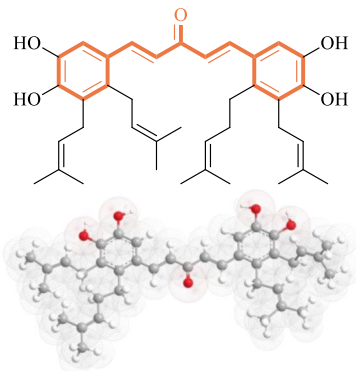
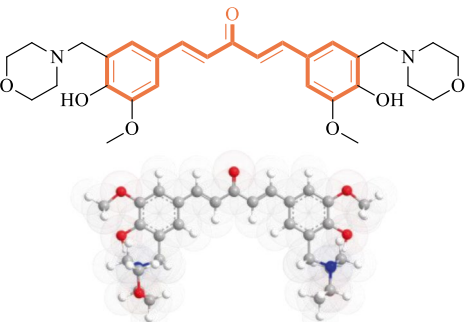
Ligand no	Compound	2D Structure and 3D Structure	Active against	Reference
DKC-18	(1E,4E)-1,5-bis(3,4-dihydroxyphenyl)penta-1,4-dien-3-one		Against various tumor: Lung tumor, Melanoma, Normal mamma tumor, Colon tumor, Renal tumor, Ovary tumor, Prostate tumor, Leukemia	[46]
DKC-19	(1E,4E)-1,5-bis(3-bromo-5-methoxy-4-((3-methylbut-2-en-1-yl)oxy)phenyl)penta-1,4-dien-3-one		Against various tumor: Lung tumor, Melanoma, Normal mamma tumor, Colon tumor, Renal tumor, Ovary tumor, Prostate tumor, Leukemia	[46]
DKC-20	(1E,4E)-1-(4,5-dihydroxy-2,3-bis(3-methylbut-2-en-1-yl)phenyl)-5-(4,5-dihydroxy-3-(3-methylbut-2-en-1-yl)-2-(4-methylpent-3-en-1-yl)phenyl)penta-1,4-dien-3-one		Against various tumor: Lung tumor, Melanoma, Normal mamma tumor, Colon tumor, Renal tumor, Ovary tumor, Prostate tumor, Leukemia	[46]
DKC-21	1,5-Bis-(4-hydroxy-3-methoxy-5-morpholin-4-ylmethylphenyl)penta-1,4-dien-3-one		against HL-60 neoplasms and HSC-2, HSC-3 and HSC-4 carcinoma cells	[47]

Table 2 (continued)

Ligand no	Compound	2D Structure and 3D Structure	Active against	Reference
DKC-22	1,5-Bis-(4-hydroxy-3-methoxy-5-pyrrolidin-1-ylmethylphenyl)-penta-1,4-dien-3-one		against HL-60 neoplasms and HSC-2, HSC-3 and HSC-4 carcinoma cells	[47]
DKC-23	1,5-Bis-[4-hydroxy-3-methoxy-5-(4-methylpiperazin-1-ylmethyl)phenyl]-penta-1,4-dien-3-one		against HL-60 neoplasms and HSC-2, HSC-3 and HSC-4 carcinoma cells	[47]
DKC-24	1,5-Bis-(3-diethylaminomethyl-4-hydroxy-5-methoxyphenyl)-penta-1,4-dien-3-one		against HL-60 neoplasms and HSC-2, HSC-3 and HSC-4 carcinoma cells	[47]
DKC-25	1,5-Bis-(4-hydroxy-3-methoxy-5-piperidin-1-ylmethylphenyl)-penta-1,4-dien-3-one		against HL-60 neoplasms and HSC-2, HSC-3 and HSC-4 carcinoma cells	[47]

Table 3 Potential binding cavities (1–5) predicted inside Er α (PDB ID: 3ERT) and aromatase (PDB ID: 3S79), as well as their volume, surface area, and location coordinates

PDB ID	Cavity no.	Volume (Å ³)	Surface area (Å ²)	Position coordinates (Å)		
				X	Y	Z
3ERT	1	364.032	844.8	34.3819	−2.28027	20.3706
	2	53.248	161.28	18.64	−0.408305	24.7403
	3	25.088	106.24	17.3088	−1.90375	3.75033
	4	14.848	60.16	8.1721	15.953	30.8405
	5	14.336	56.32	27.2598	10.9126	−0.119061
3S79	1	96.256	204.8	85.7363	53.9369	45.8998
	2	93.184	362.24	73.3086	46.6916	32.4541
	3	68.096	244.28	83.5399	52.4483	58.6364
	4	59.392	202.24	94.9193	35.4838	36.3966
	5	39.936	161.28	70.1335	58.2242	49.4988

were loaded into MVD's pre-saved workspace, with the optimized aromatase and Er α having an anticipated binding cavity. For docking with 25 deketene curcumin derivatives and currently available medications, the most plausible aromatase (cavity 1) and Er α receptor (cavity 1) binding sites were chosen. The 30 Å grid resolution was set during the docking process, and then 10 runs and the population size of 50 were chosen for operating molecular docking simulation; this can be done by the usage of MolDock Simplex Evolution search algorithm [48]. Here, the term number of runs means the number of docking simulations that were run for each ligand that was docked, with each iteration returning to a single final solution, for instance, pose. This process in the software was done by a special algorithm in which a 12–6 conceivable and sp²–sp² torsion by Lennard Jones term was used [49]. Based on pilot docking findings, re-rank scores were determined for rating the inhibitor poses in the MolDock, and the poses chosen as the best for all of the deketene curcumin derivatives and current medicines were evaluated here. Further, default parameters were selected for maximum iteration (1500), threshold (100), binding radius (20 Å), SE maximum steps (300), and SE neighboring distance factor (1.00). For the study of binding interactions like hydrogen bonding and steric interaction, the best conformer or pose of the ligand was selected, which has the lowest MolDock score [50].

The binding affinity or MolDock score can be determined by the utilization of differential evolution algorithm. Here, Eq. 1 describes the total binding affinity or MolDock score (E_{score}), and the terms used in this equation are E_{inter} which shows the ligand and receptor energy interaction and E_{intra} which depicts the ligand internal energy. Furthermore, to calculate the E_{inter} and E_{intra} , Eqs. 2 and 3 are utilized

correspondingly. Despite this, piecewise linear potential (E_{PLP}) was used to check the steric interaction among the atoms which are charged [48, 51, 52].

$$E_{\text{score}} = E_{\text{inter}} + E_{\text{intra}} \quad (1)$$

$$E_{\text{inter}} = \sum_{i=\text{ligand}} \sum_{j=\text{protein}} \left[E_{\text{PLP}}(r_{ij}) + 332.0 \frac{q_i q_j}{4r_{ij}^2} \right] \quad (2)$$

$$E_{\text{intra}} = \sum_{i=\text{ligand}} \sum_{j=\text{protein}} [E_{\text{PLP}}(r_{ij})] + \sum_{\text{flexible bond}} A[1 - \cos(m\theta - \theta_0)] + E_{\text{clash}} \quad (3)$$

The first term in Eq. 3 describes the energy of the ligand's pair of atoms; however, this is only valid for a single bond. The torsional energy has been depicted by the second term of the equation, in that the torsional angle of the bond is denoted by θ . The average of the torsional energy can be taken if the number of torsions would determine. The third term which is E_{clash} is used when the distance among 2 dense atoms is lesser than 2.0 Å and allotting penalty of 1000 kcal/mol [48]. Apart from this, Molegro Virtual Docker (MVD) is suggested by various scientists because, if compared to specific accessible docking programs, MVD has great accuracy (MD: 87%, Glide: 82%, Surflex: 75%, FlexX: 58%) and has been tested to be worthwhile in several recent studies; additionally, this program is less costly and produces docking results in less time [48]. The binding of ligands by molecular docking (deketene curcumin derivatives) and protein was visualized using Molegro Molecular Viewer 7.0.0 (MMV) (AIs and Er α). It is software for studying and simulating molecular protein–ligand interactions, sequences, and structures.

ADME/pharmacokinetics studies

The antagonistic response of an inhibitor to an enzyme or a protein receptor does not guarantee its suitability as a

Fig. 4 MVD detects five active sites in the protein structure of (a) aromatase and (b) Er α (PDB ID: 3S79, 3ERT) (cavity volume shown in \AA^3). Detected cavity representation: color with specifications, green, cavity; blue (β sheets); and red (α helices). Cartoon models of aromatase (a) and Er α (b): yellow, binding ligand

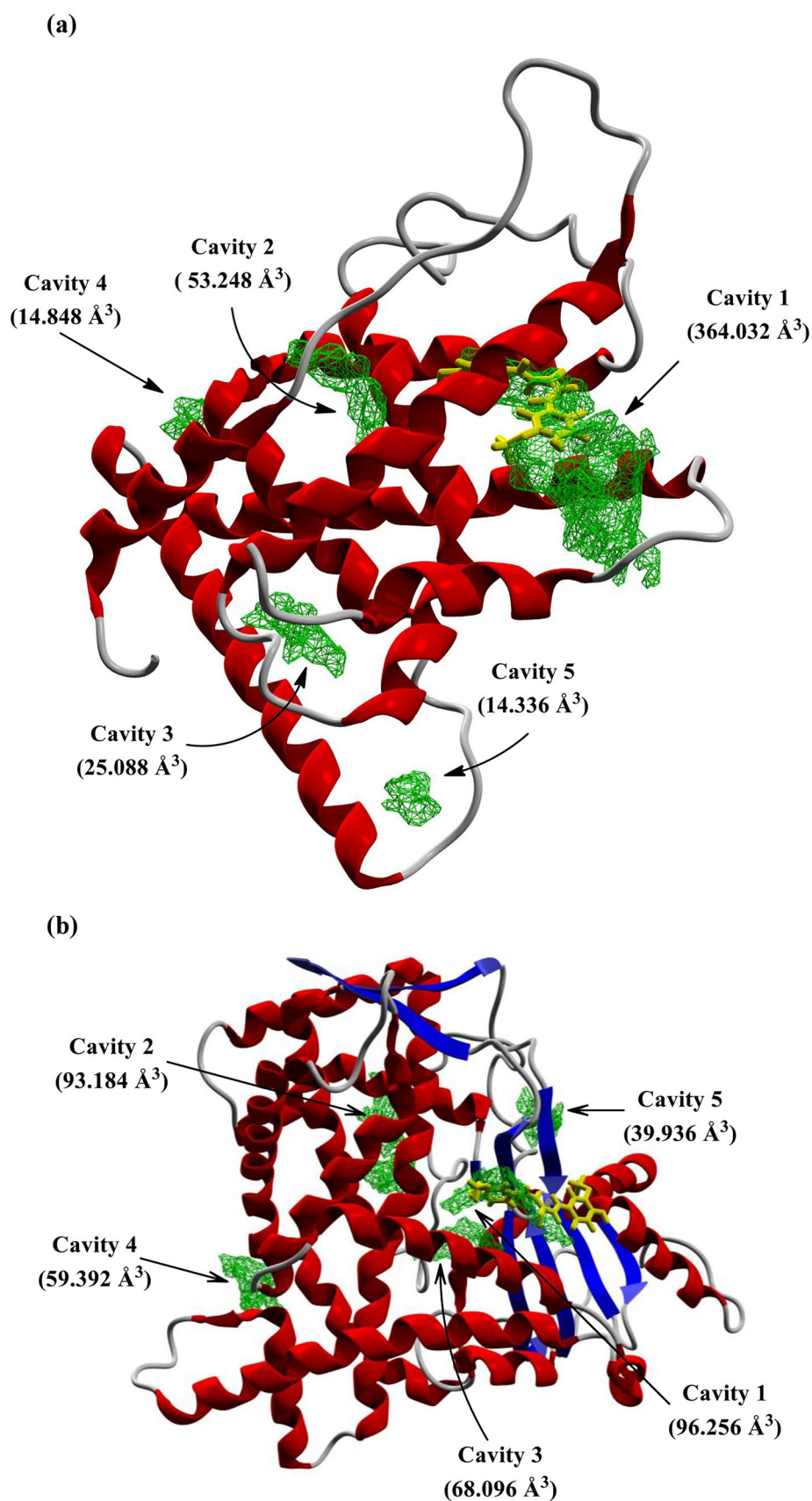


Table 4 Drug likeness and ADME/Pharmacokinetics data of DKC derivatives

Ligand no.	nHA	nAHA	SA	GI	BBB	Pgp	MR	BS
DKC-1	24	12	2.76	High	Yes	No	92.99	0.55
DKC-2	34	12	3.91	High	No	No	139.44	0.55
DKC-3	28	12	3.40	High	No	No	106.50	0.55
DKC-4	32	12	4.51	High	Yes	Yes	125.34	0.55
DKC-5	28	12	3.14	High	No	No	105.97	0.55
DKC-6	32	12	3.59	Low	No	Yes	115.66	0.55
DKC-7	36	12	3.94	Low	No	Yes	128.64	0.17
DKC-8	34	12	3.88	High	No	No	125.49	0.55
DKC-9	24	12	2.76	High	Yes	No	92.99	0.55
DKC-10	62	17	7.70	High	No	Yes	247.92	0.17
DKC-11	38	12	4.32	High	No	Yes	144.72	0.55
DKC-12	34	12	3.77	High	No	No	125.80	0.55
DKC-13	46	12	5.13	High	No	Yes	168.29	0.17
DKC-14	29	12	3.55	High	Yes	No	106.79	0.55
DKC-15	31	12	-	-	-	-	117.38	-
DKC-16	34	12	4.00	High	No	No	140.43	0.55
DKC-17	31	12	-	-	-	-	117.38	-
DKC-19	22	12	2.56	High	No	No	84.05	0.55
DKC-20	36	12	4.12	High	No	No	154.84	0.17
DKC-21	38	12	3.98	High	No	Yes	152.61	0.55
DKC-22	36	12	3.77	High	No	Yes	150.77	0.55
DKC-23	40	12	4.29	High	No	Yes	174.01	0.55
DKC-24	36	12	4.02	High	No	No	147.17	0.55
DKC-25	38	12	3.99	High	No	Yes	160.38	0.55
Ligand no.	MW (g/mol)	nHBA	nHBD	nRot	TPSA (Å)	iLOGP	WLOGP	nLV
DKC-1	326.34	5	2	6	75.99	3.10	3.19	0
DKC-2	462.58	5	0	12	53.99	5.54	6.47	0
DKC-3	374.30	6	2	6	106.50	3.26	3.97	0
DKC-4	434.52	5	0	8	53.99	4.67	5.58	0
DKC-5	386.40	7	2	8	94.45	3.47	3.21	0
DKC-6	484.50	11	2	10	191.07	2.11	3.11	1
DKC-7	544.55	13	2	12	209.53	2.85	3.13	2
DKC-8	474.50	9	0	16	90.91	4.79	3.70	0
DKC-9	326.34	5	2	6	75.99	3.10	3.19	0
DKC-10	879.07	12	3	30	207.92	7.18	5.81	1
DKC-11	530.61	9	0	20	90.91	5.55	3.87	1
DKC-12	474.50	9	4	16	134.91	3.87	1.25	0
DKC-13	650.71	13	0	28	127.83	6.31	3.76	2
DKC-14	398.41	7	0	10	72.45	4.13	3.46	0
DKC-15	421.44	7	2	9	109.01	-	4.01	0
DKC-16	462.58	5	2	10	75.99	4.98	6.21	0
DKC-17	421.44	7	2	9	109.01	-	4.01	0
DKC-19	298.29	5	4	4	97.99	1.95	2.59	0
DKC-20	620.37	5	0	12	53.99	6.09	8.00	1
DKC-21	524.61	9	2	10	100.93	4.68	1.79	1
DKC-22	492.61	7	2	10	82.47	4.50	3.32	0
DKC-23	550.69	9	2	10	88.95	5.18	0.86	1
DKC-24	496.64	7	2	14	82.47	5.56	4.57	0
DKC-25	520.66	7	2	10	82.47	5.16	4.10	1

nHA number of heavy atoms, *nAHA* number of aromatics heavy atoms, *SA* synthetic accessibility, *GI* gastrointestinal absorption, *BBB* blood–brain barrier permeant, *Pgp* P-glycoprotein substrate, *MR* molecular refractivity, *MW* molecular weight, *nHBD* number of hydrogen bond donor, *nHBA* number of hydrogen bond acceptor, *nRot* number of rotatable bonds, *BS* bioavailability score, *TPSA* topological polar surface area, *WLOGP* water partition coefficient, *nLV* number of Lipinski violation

Table 5 Re-rank score, MolDock score, H-bonding, and steric score of DKC derivatives and reference drugs against breast cancer (PDB: 3ERT, 3S79)

Molecule ID	Energy, kcal/mol or MolDock score		H-bond energy, kcal/mol		Re-rank score, kcal/mol		Steric interaction, kcal/mol	
	3ERT	3S79	3ERT	3S79	3ERT	3S79	3ERT	3S79
DKC-1	-125.271	-98.215	-7.4962	-4.5464	-74.572	-68.455	-123.575	-98.9423
DKC-2	-133.508	-125.636	-2.5	-6.76856	-9.1031	-89.6765	-145.761	-128.249
DKC-3	-137.941	-114.793	-9.12268	-4.2454	-88.4477	-75.1558	-134.165	-117.102
DKC-4	-113.949	-106.079	-2.5	-0.89985	-77.9106	-68.1176	-143.671	-140.282
DKC-5	-134.157	-136.674	-2.5	-7.94795	-94.8894	-90.0729	-131.456	-132.22
DKC-6	-131.674	-122.867	-2.57617	-5.18398	-105.322	-92.1571	-138.746	-128.792
DKC-7	-125.954	-130.992	-3.32824	-9.9252	-43.9204	-90.4882	-132.621	-131.149
DKC-8	-148.539	-147.973	-2.5	-7.89019	-113.932	-108.531	-153.558	-155.691
DKC-9	-123.696	-105.285	-4.74606	-3.41067	-84.4248	-76.8949	-121.306	-108.801
DKC-10	-204.461	-201.613	-2.00227	-4.39591	-145.249	-97.6856	-203.763	-196.119
DKC-11	-146.079	-130.689	-0.53985	-3.08584	-107.493	-89.2058	-165.696	-152.037
DKC-12	-157.412	-158.587	-1.96659	-13.1848	-113.297	-92.6956	-157.059	-145.458
DKC-13	-159.765	-110.715	-5.04032	-5.46182	-113.464	-59.2572	-190.221	-150.971
DKC-14	-133.237	-113.319	-1.81773	-4.90099	-45.2329	-57.4149	-146.541	-115.485
DKC-15	-135.859	-121.952	-9.16905	-7.54186	-83.4043	-66.3515	-143.214	-107.867
DKC-16	-160.714	-124.673	-2.39095	-5	-120.856	-66.5945	-165.265	-131.833
DKC-17	-139.024	-108.898	-4.52467	-6.12468	-49.5062	-52.4709	-151.536	-116.135
DKC-18	-125.777	-101.112	-11.7255	-17.6283	-65.7571	-72.3188	-116.385	-91.6254
DKC-19	-137.71	-110.297	-1.10284	-3.26476	-102.283	-63.5474	-153.08	-140.148
DKC-20	-177.278	-131.397	-2.66189	-6.86614	-123.461	-50.1625	-178.181	-121.53
DKC-21	-161.958	-123.724	-3.91206	-3.7796	-124.815	-87.4512	-174.608	-142.2
DKC-22	-161.134	-141.476	-1.43387	-3.72418	-113.364	-94.3325	-163.614	-149.009
DKC-23	-160.562	-126.371	-2.43209	-1.74234	-120.324	-68.7802	-169.038	-141.165
DKC-24	-157.876	-125.901	-3.19185	-1.96174	-105.475	-43.6616	-167.746	-138.8
DKC-25	-157.588	-133.383	-2.5	-3.67551	-117.746	-77.3043	-175.356	-154.761
Tamoxifen	-131.909	-	0	-	-100.876	-	-141.13	-
Anastrozole	-	-107.965	-	-1.81796	-	-73.5789	-	-109.76
Exemestane	-	-92.7947	-	-2.85662	-	-68.4719	-	-83.4808
Letrozole	-	-108.904	-	-6.36	-	-74.7362	-	-110.994

potential drug [53]. As a result, ADME (absorption, distribution, metabolism, and excretion) analysis and drug-likeness analysis have been critical in drug discovery because they aid in making the correct decision about whether or not to evaluate inhibitors against a biological system [53, 54]. Additionally, the majority of failed medications in clinical trials were produced by inhibitors with insufficient ADME properties, causing severe damage to biological systems as a result of the excessive toxicity. Additionally, the ADME study was conducted via the Swiss ADME web server (Swiss Institute of Bioinformatics, Switzerland). The selected 25 deketene curcumin derivatives are then imported into the program via SMILES (Simplified Molecular Input Line Entry System) in order to generate a pharmacokinetic profile or drug-likeness specification [55].

Apart from that, a specific rule has been established to determine whether or not an inhibitor with specific medical and pharmacological characteristics is a safe and orally active medication in the human body. Christopher A. Lipinski developed a thumb rule for determining drug-likeness in 1997. Additionally, the rule of five (5) may be referred to as Pfizer's rule of five (5) or Lipinski's rule of five (5) [54]. As per this rule, if two (2) or more of these thresholds are met, a drug could be orally absorbed into the human body. These cut-offs are as follows: the MW (molecular weight) of the molecule should be less than 500 g/mol, iLOGP (octanol/water partition coefficient) should be ≤ 5 , then the nHBD (H-bond donor) and nHBA (H-bond acceptor) should be in the range of ≤ 10 and ≤ 5 , respectively, and further, the TPSA (topology polar surface area) should be 40 \AA^2 [56, 57]. Table 4 illustrates the

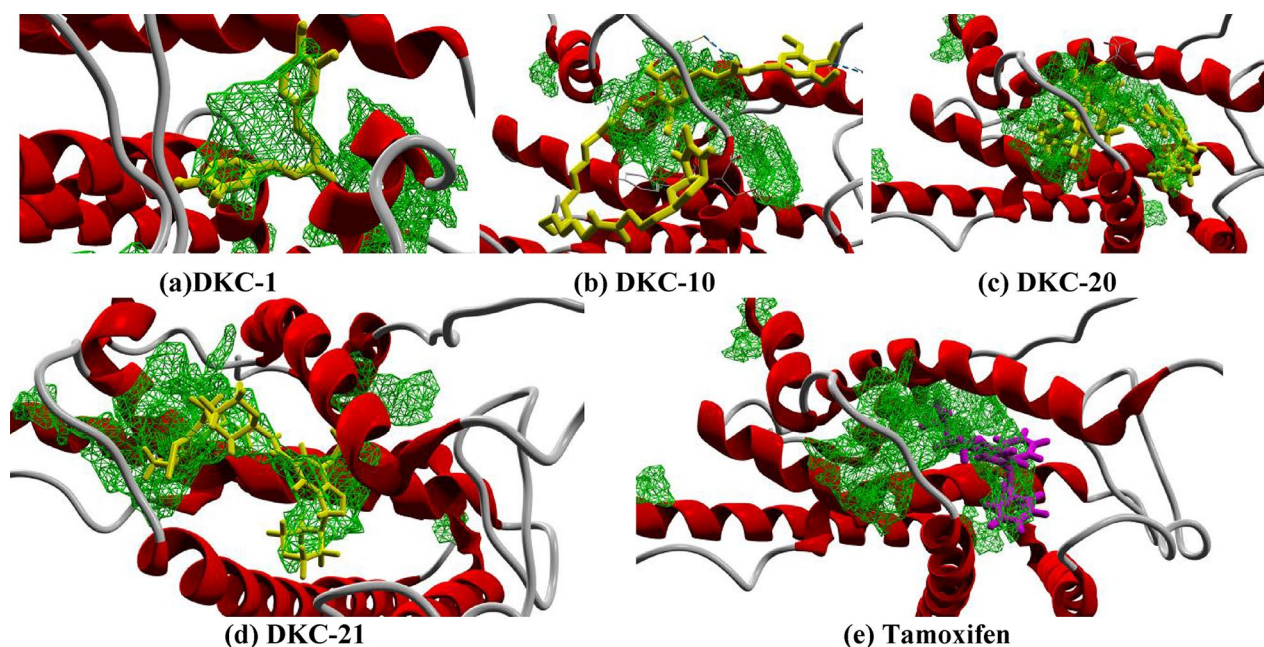


Fig. 5 Docking interaction of 4 DKC ligands and tamoxifen with $Er\alpha+$ (PDB: 3ERT). (a–d) DKC-1, 10, 20, and 21 in stick line, yellow color; protein back bone, red color (α helices); and cavity, green color and (e) tamoxifen in pink color with same protein specifications

drug-like data of deketene curcumin and its derivatives. If these cut-off values correspond to the respective drug, there will be no violation of the Lipinski rule.

Result and discussion

In present work, 25 DKC compounds were successfully docked to the human placental aromatase cytochrome p450 and $Er\alpha+$ receptor in this study (PDB ID: 3S79, 3ERT, respectively). Additionally, a comparative docking study was conducted using currently used drugs (tamoxifen, anastrozole, exemestane, and letrozole) to treat breast cancer. As previously stated and as determined through the literature, tamoxifen is an antagonist type of drug (study conducted on $Er\alpha+$), whereas the other three are AI type of drugs (study conducted on aromatase); thus, different PDBs were used for the comparative study. Moreover, the best poses were selected to calculate the MolDock and re-rank scores while performing the docking study. Here, Table 5 represents the MolDock score, H-bonding, re-rank score, and steric score between protein of breast cancer and ligand (DKC derivatives and 4 drugs). In addition to this, through literature it was confirmed that ligands (DKC-10, DKC-20, and DKC-21 for $Er\alpha+$) which are exhibited binding

affinity less than -150 kcal/mol would be regarded as a more effective inhibitor [40–48]. In this study, 3 deketene curcumin derivatives (DKC-10, DKC-20, and DKC-21) out of 25 have been abstracted for depth explanation as these derivatives elicit better binding energy (for $Er\alpha+$ -204.461 kcal/mol, -177.278 kcal/mol, and -161.958 kcal/mol, respectively, for aromatase, -201.613 kcal/mol, -131.397 kcal/mol, and -123.724 kcal/mol correspondingly), re-rank score, and H-bonding. The MolDock scores of DKC derivatives exhibited good energy in comparison with core DKC-1; the core DKC-1 has been taken for comparison among selected 3 ligands. Apart from this, other 21 ligands of DKC derivatives show optimum binding affinity in comparison with DKC-1. Despite this, three DKC derivative activities in terms of binding affinity on aromatase are low as compared to estrogen receptor.

Furthermore, cartoon representations of the binding interaction between ligand and protein have been included in Figs. 5 and 6. Docking results indicate that DKC-10 has the highest MolDock score, H-bonding, and steric interaction with the estrogen and aromatase protein structures, in comparison to other DKC derivatives. Tables 6 and 7 and Figs. 7 and 8 illustrate the H-bonding and steric interaction of the DKC-1, DKC-10, DKC-20, and DKC-21 with $Er\alpha+$. Similarly, the aromatase's ligand interactions are

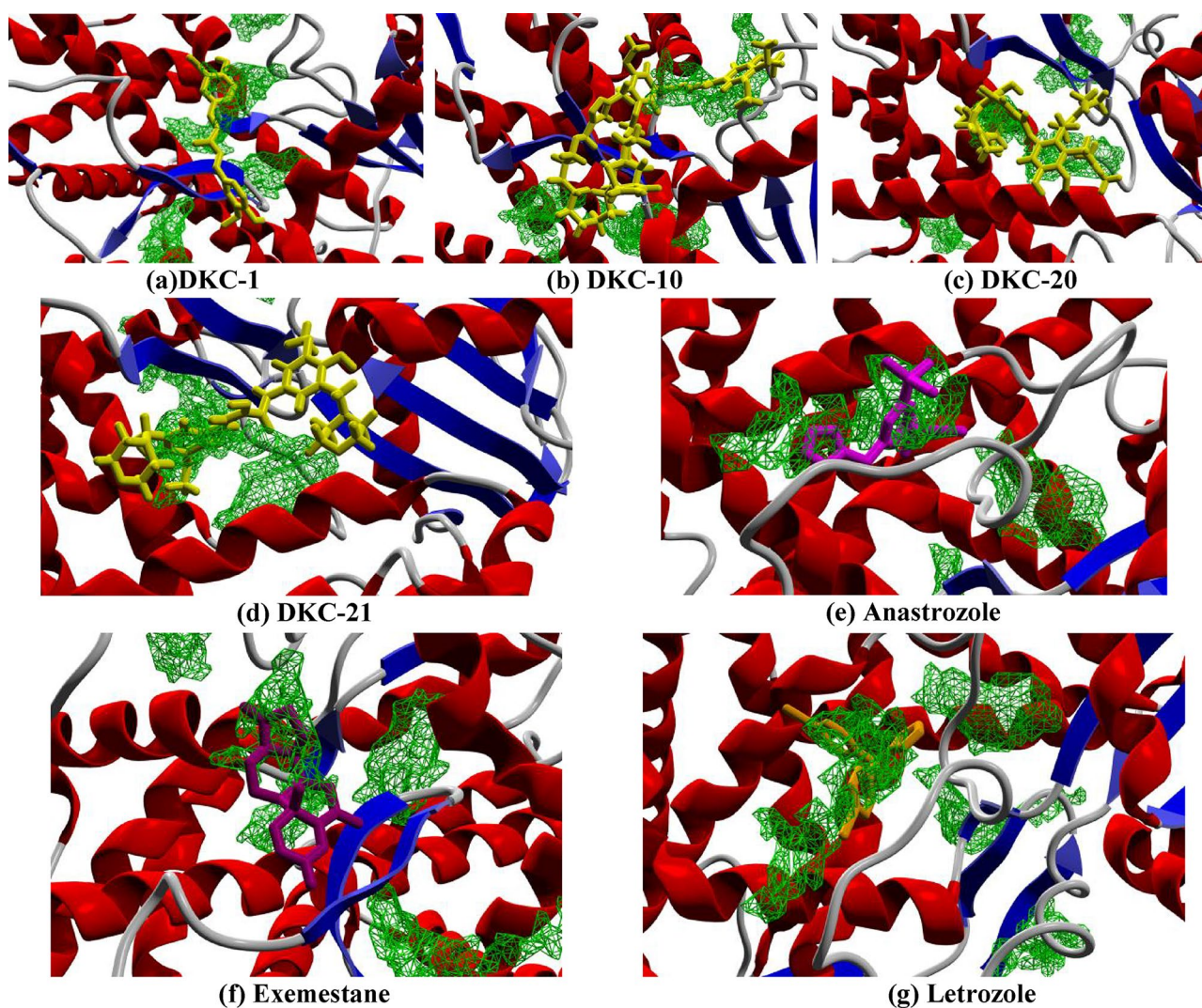


Fig. 6 Docking interaction of 4 DKC ligands, anastrozole, exemestane, and letrozole with aromatase (PDB: 3S79). (a–d) DKC-1, 10, 20, and 21 in stick line, yellow color; protein back bone, red color (α

helices) and blue (β -sheets); and cavity, green color, (e) anastrozole, (f) exemestane, and (g) letrozole in pink, purple, and orange color, respectively, with same protein specifications

depicted in Tables 8 and 9 and Figs. 9 and 10. Additionally, these tables and figures include interactions for the reference drugs.

To begin with, a depth description of each of these ligand's hydrogen and steric interaction with $E\alpha$ + and aromatase has been discussed. First, DKC-1 forms H-bond with $E\alpha$ + and aromatase by binding with amino acids His 524, Gly 521, Gly 420, Thr 347, Leu 387, Arg 394 and Arg 403, Tyr 366, Gln 367, Met 68, Ser 72, and His 475, respectively. In the case of estrogen receptor H-bonding, the interacting atoms (O (24), O(25) of the hydroxyl functional group, then

atoms O (22), O (15) of the methoxy group, and atoms O (6) of the carbonyl group responsible for H-bonding) of DKC-1 ligand with corresponding amino acids (Gly 521, Gly 420, Leu 387, His 524, Arg 394 and Thr 347) (Fig. 7a). Similarly, for H-bonding in aromatase by DKC-1, the same functional groups except carbonyl are involved with binding residues and ligand atoms which are Ser 72 with O(24), Met 68 with O(24), and Tyr 366 with O(15) for hydroxyl and His 475, Arg 403, and Gln 367 for methoxy group; here noticeable observation can be seen that the same interacting oxygen atom number “O(15)” for methoxy group is involved for all the

Table 6 Properties of H-bond interaction between top three docking poses of DKC derivative and tamoxifen with PDB ID: 3ERT

Molecule ID	Interacting amino acid	Interacting protein atom	Interaction energy (Kcal/mol Å)	Interaction distance in Å	Interacting ligand atom	H-bond donor
DKC-1	His 524	ND1	-1.06361	2.60078	O(22)	Target His 524
	Gly 521	O	-0.177186	3.43158	O(24)	Ligand
	Gly 420	O	-2.5	2.73288	O(24)	Ligand
	Thr 347	OG1	-0.541066	3.49179	O(6)	Target Thr 347
	Leu 387	O	-2.5	2.67695	O(15)	Ligand
	Arg 394	NH2	-0.531065	3.4439	O(15)	Target Arg 394
DKC-10		NH2	-0.606492	3.30652	O(13)	Target Arg 394
	Ser 341	OG	-2.50	3.06037	O(21)	Ligand
	Cys 530	SG	-2.5	3.05687	O(4)	Target Cys 530
	Leu 536	N	-1.22659	3.34801	N(35)	Target Leu 536
	Tyr 526	OH	-0.26233	3.41327	N(48)	Ligand
DKC-20		N	-0.833286	2.74917	N(61)	Ligand
	Leu 346	O	-1.09214	3.38157	O(24)	Ligand
	Glu 353	OE2	-2.50	2.7854	O(24)	Ligand
DKC-21	Thr 347	OE2	-2.0007	3.19986	O(6)	Target Thr 347
	His 524	ND1	-0.991925	3.30934	O(33)	Target His 524
	Cys 530	SG	-1.85514	3.22897	O(22)	Target Cys 530
Tamoxifen		N	-0.420038	3.09516	O(22)	Target Cys 530
	Met 528	O	-2.5	3.0453	O(22)	Ligand
	Thr 347	OG1	-2.5	2.98053	O(6)	Target Thr 347

amino acids (Fig. 8a) (Tables 6 and 8). Apart from this, steric interaction can be observed in both the proteins (E α + and aromatase) and amino acids which involved in it are Met 343, Glu 419, Gly 521, Gly 420, Thr 347, Phe 404, Leu 346, Glu 353, Ala 350, Leu 387, Leu 349 and His 475, Gln 367, Lys 473, Tyr 366, and Met 68, respectively. Here, it can be observed that more number of residues are involved for binding with E α + in steric interactions as compared to aromatase (Figs. 9a and 10a, Tables 7 and 9). In addition to this, steric interactions of DKC-10 ligand with both the proteins have been illustrated in Figs. 9b and 10b. The involving residues for steric interactions are Ser 341, Cys 530, Leu 536, and Tyr 526 for estrogen receptor while Arg 400, Arg 79, Leu 479, Arg 403, His 475, Lys 473, Met 68, Trp 67, and Ser 72 for aromatase. Besides this, as per Figs. 7b and 8b, the H-bonding interactions are observed between DKC-10 ligand and subsequent protein structures of E α + and aromatase. Here, in DKC-10, H-bonding interaction with estrogen receptor consists of amino acids binding with the interacting atom of respective functional groups which are Ser 341 with O(21) of -OCH₃ group, Cys 530 with O(4) of -C=O group, Leu 536 with N(35) of triazole moiety, and Tyr 526 with N(48) of -NH group (Fig. 7b),

whereas in H-bonding between DKC-10 and aromatase, the interacting atoms O(12), O(12), O(51), O(62), and N(48) of the functional groups -OCH₃, -C=O, and -NH correspondingly are present with subsequent amino acids which are Arg 79, Arg 400, Ser 72, Trp 67, and Lys 413 (Fig. 8b).

On the other hand, the ligand DKC-20 forms a hydrogen bond with E α + via interactions between residues Leu 346 and Glu 353, which interact with the hydroxyl group's atom number O(21), and then Thr 347 interacts with the carbonyl group's atom number O(6) (Fig. 7c). In the case of DKC-20 H-bonding interaction with aromatase, Pro 481, His 480 with interacting atom number O(42), Glu 483, Arg 192 with interacting atom number O(43), Lys 243, Tyr 249 with interacting atom O(24), the ligand's lone common functional group, "-OH," is responsible for hydrogen bonding (Fig. 8c). In addition, the steric interactions of this ligand with both the proteins have been illustrated in Figs. 9c and 10c, in which involving amino acids are Leu 349, Ala 350, Leu 346, Met 388, Met 421, Met 343, His 524, and Trp 383 for E α + interaction with DKC-20, while Lys 230, Tyr 244, Asp 222, Gln 218, Phe 221, Glu 483, Pro 481, and His 480 for aromatase interaction. Moreover, the steric interaction in DKC-21 ligand with E α + and aromatase is depicted

Table 7 Properties of steric interaction between top three docking poses of DKC derivative and tamoxifen with PDB ID: 3ERT

Molecule ID	Interacting amino acid	Interaction distance in Å	Strength	Interacting ligand atom	
DKC-1	Met 343	2.47	5.00	C(23)	
	Glu 419	3.19	0.68	C(23)	
	Gly 521	3.02	1.69	O(24)	
		2.99	1.86	C(20)	
	Gly 420	3.30	0.02	C(23)	
	Thr 347	3.14	0.96	O(6)	
	Leu 346	3.06	1.46	C(4)	
	Phe 404	3.29	0.06	C(14)	
	Glu 353	3.24	0.39	O(13)	
	Ala 350	3.17	0.81	C(4)	
	Leu 387	3.00	1.79	C(11)	
	Leu 349	3.03	1.65	C(14)	
	DKC-10	Gly 344	3.03	1.65	O(22)
			2.53	4.66	O(21)
3.22			0.48	C(27)	
Ser 341		3.25	0.27	C(27)	
Met 528		3.28	0.14	O(4)	
		3.13	1.04	O(4)	
Cys 530		3.19	0.67	C(13)	
		3.03	1.64	C(13)	
		2.95	2.10	C(13)	
Leu 536		3.12	1.11	N(35)	
Lys 529		3.14	0.36	C(29)	
Glu 380		3.24	0.35	N(34)	
Ser 527		3.16	0.84	C(57)	
Tyr 526		3.24	0.39	C(58)	
DKC-20	Leu 349	3.25	0.29	C(49)	
		2.63	4.09	C(49)	
	Leu 349	3.23	0.41	O(24)	
	Ala 350	2.78	3.18	C(12)	
	Leu 346	2.55	4.52	C(12)	
	Met 388	3.27	0.18	C(22)	
	Met 421	2.63	4.06	C(23)	
	Met 343	3.30	0.03	C(15)	
	His 524	3.16	0.86	C(17)	
	Trp 383	2.89	2.48	O(42)	
DKC-21	Asp 351	2.87	2.59	O(6)	
	Gly 420	3.22	0.46	C(32)	
		3.30	0.02	O(20)	
	Leu 525	3.17	0.78	C(34)	
		3.30	0.02	O(20)	
	Met 421	3.11	1.17	C(31)	
	Met 343	3.10	1.21	C(29)	
	Ala 350	3.26	0.25	C(2)	
Tamoxifen	Met 421	3.25	0.32	C(23)	
	Phe 404	3.30	0.01	C(16)	
	Asp 351	2.82	2.91	C(3)	
		3.30	0.01	N(2)	

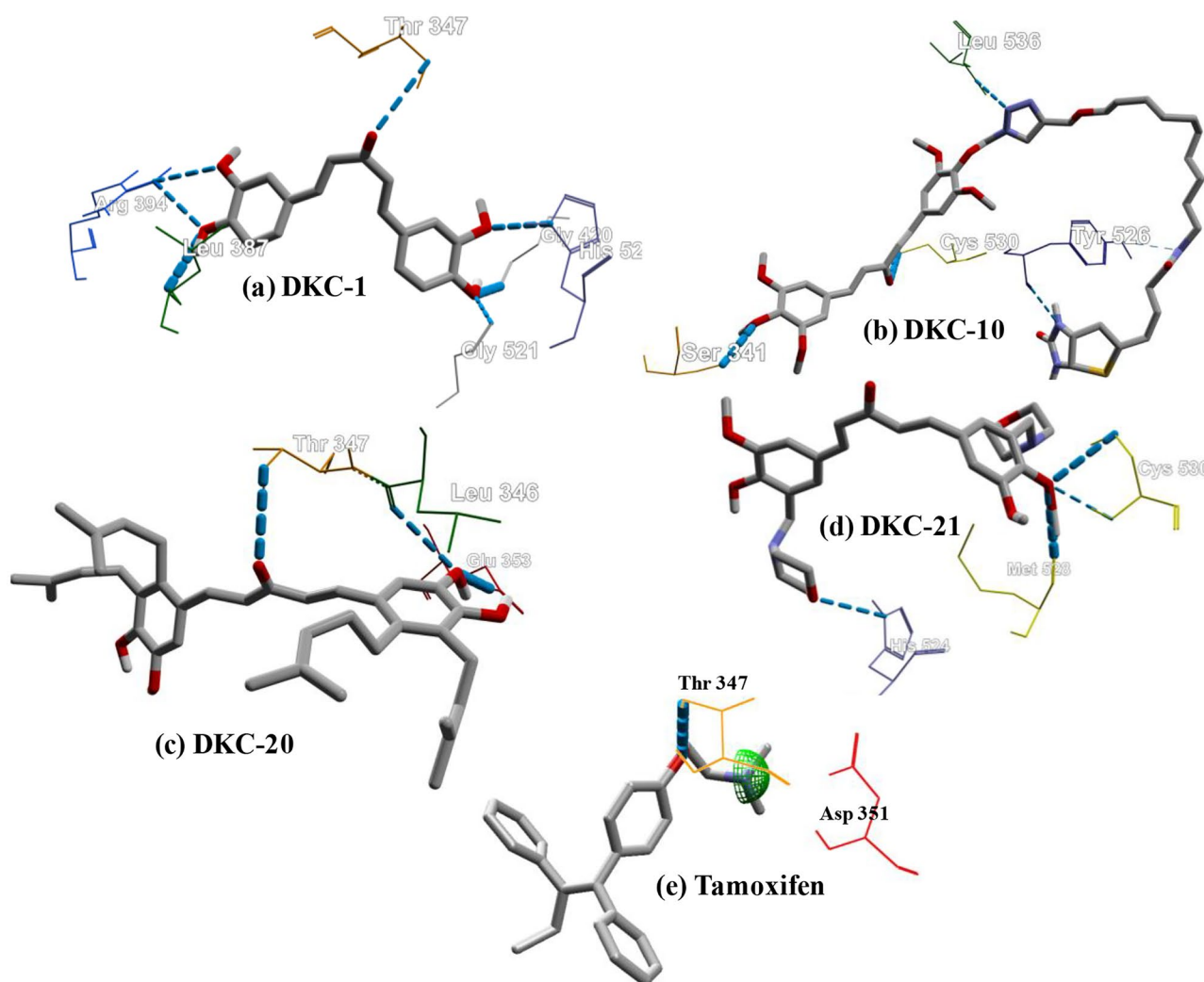


Fig. 7 H-bond interactions (blue-dotted bonds) displayed between 4 DKC ligands and tamoxifen with $Er\alpha$ +PDB ID: 3ERT. (a–d) DKC-1, 10, 20, and 21 hydrogen bonding interaction with estrogen receptor and (e) tamoxifen hydrogen bonding with $Er\alpha$ +

in Figs. 9d and 10d; the interacting amino acids are Asp 351, Gly 420, Leu 525, Met 421, Met 343, Ala 350 and Glu 218, Glu 483, Asp 222, Ile 474, Glu 225, Ala 226, and Met 68, respectively. Apart from this, H-bonding of DKC-21 with $Er\alpha$ can be seen in Fig. 7d, in which ylmethylphenyl group of the ligand interacts with His 524 amino acid with the interacting atom number O(33), and then Cys 550 and Met 528 interact with –OH group of the ligand with interacting atom number O(22). While, in the case of DKC-21, the H-bonding interaction with aromatase involves amino acids (Lys 230, Tyr 244) binds with atom O(33) of the ligand, and amino acid (Glu 218) binds with atom O(6) of the ylmethylphenyl group, the amino acid (Leu 230 and Trp 67) binds with the oxygen atom of O(38) number of the hydroxyl group. Similarly, amino acids (Arg 192 and Glu 483) binds with the oxygen atom [O(22)] of the –OH group.

After the comprehensive discussion of the interactions of DKC derivatives, it was observed that DKC-10 ligand exhibits the highest MolDock score (–204.461 kcal/mol with $Er\alpha$ + and –201.613 kcal/mol with aromatase) against the breast cancer. This is due to the strong H-bond and steric interactions, as well as the shorter interacting distance. Additionally, other supporting data for hydrogen bonding and steric interaction, such as interacting distance, interaction energy, strength, and the H bonding donor atom between the ligand and protein, are well represented in Tables 6, 7, 8, and 9.

In this study, we also did a comparison analysis (Tables 10 and 11), in which we evaluated the drugs that are presently used to treat breast cancer. First, the interactions of tamoxifen (antagonist type drug) has been evaluated

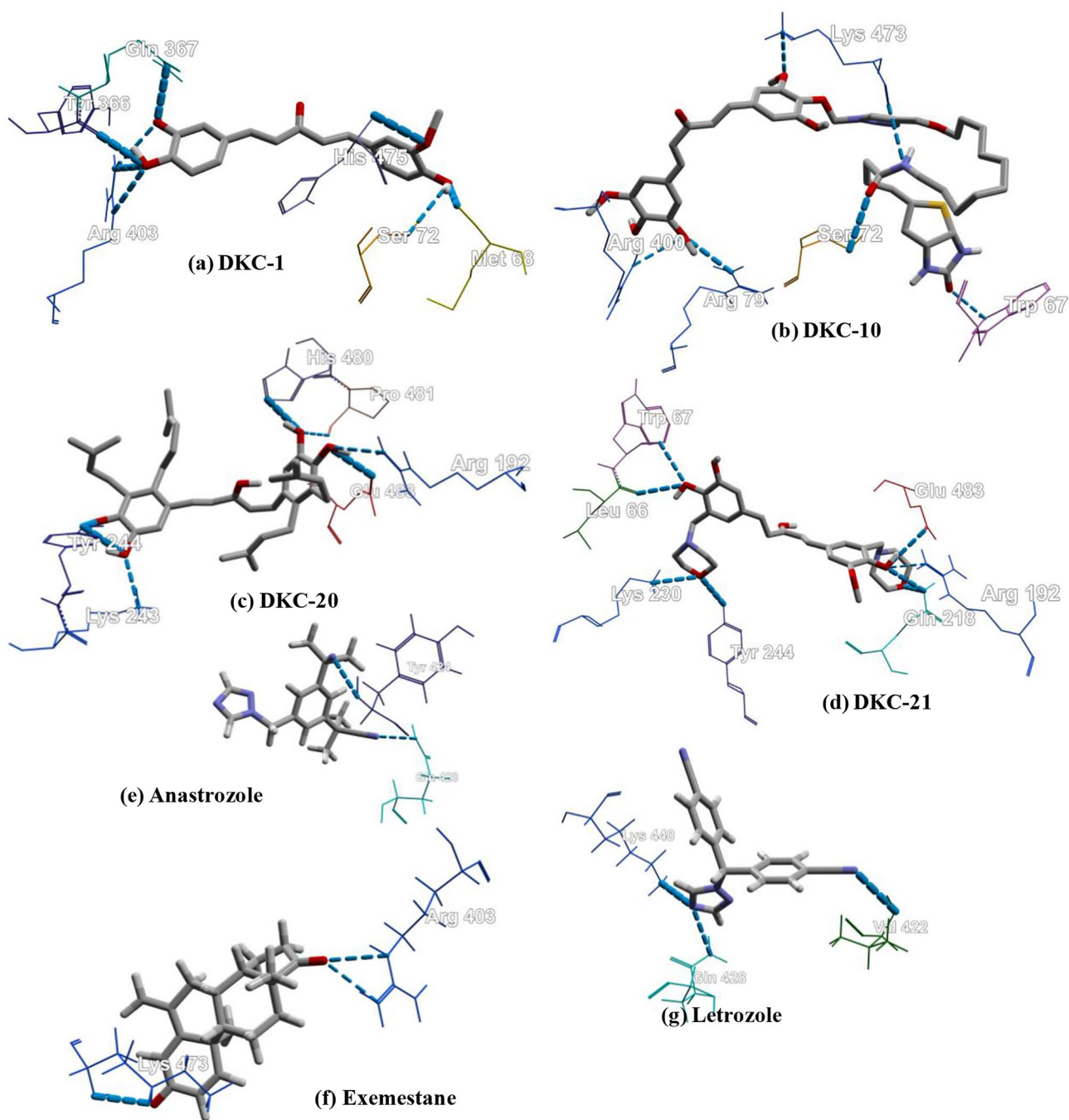


Fig. 8 H-bond interactions (blue-dotted bonds) displayed between 4 DKC ligands and 3 drugs with aromatase PDB ID: 3S79. (a–d) DKC-1, 10, 20, and 21 hydrogen bonding interaction with aromatase and (e–g) exemestane, anastrozole, and letrozole hydrogen bonding with aromatase

Table 8 Properties of H-bond interaction between top 3 docking poses of DKC derivative and exemestane, anastrozole, and letrozole with PDB ID: 3S79

Molecule ID	Interacting amino acid	Interacting protein atom	Interaction energy (Kcal/mol Å)	Interaction distance in Å	Interacting ligand atom	H-bond donor
DKC-1	Arg 403	NH2	-2.11469	2.81011	O(15)	Arg 403
		NH2	-0.680609	3.20804	O(13)	Arg 403
	Tyr 366	O	-2.5	2.60305	O(15)	Ligand
	Gln 367	NE2	-2.5	2.77063	O(13)	Gln367
	Met 68	O	-1.95123	2.53415	O(24)	Ligand
	Ser 72	OG	-0.709929	3.45801	O(24)	Ligand
DKC-10	His 475	N	-2.5	3.0684	O(22)	His 475
		Arg 79	NH1	-1.50535	3.29893	O(12)
	Arg 400	NH1	-1.98122	3.20376	O(12)	Arg 400
	Ser 72	O	-2.5	3.05591	O(51)	Ser 72
	Lys 473	O	-0.866787	3.32424	N(48)	Ligand
		N	-2.5	2.82116	O(20)	Lys 473
DKC-20	Trp 67	NE1	-0.515552	2.60534	O(62)	Tyr 67
		Lys 243	N	-1.0294	3.39412	O(24)
	Tyr 244	OH	-2.5	2.98727	O(24)	Both
		OH	-2.5	2.69089	O(25)	Both
	Pro 481	O	-0.416259	2.34995	O(42)	Ligand
	His 480	NE2	-2.5	2.70549	O(42)	Ligand
DKC-21	Arg 192	NH2	-0.734587	3.33627	O(43)	Target Arg 192
		Glu 483	OE1	-2.5	2.92788	O(43)
	Gln 218	NH2	-0.189517	3.35792	O(22)	Target Arg 192
		NE2	-1.78868	3.24226	O(22)	Target Gln 218
	Glu 483	NE2	-2.19014	3.16197	O(17)	Target Gln 218
		OE1	-1.49575	3.30085	O(22)	Ligand
Anastrozole	Tyr 244	OH	-2.5	3.09962	O(33)	Target Tyr 244
		Lys 230	N	-1.69385	3.26123	O(33)
	Try 67	O	-1.31209	3.33785	O(38)	Ligand
		O	-1.7352	3.25396	O(38)	Ligand
	Gln 428	NE2	-2.5	3.0995	N(8)	Gln 428
		N	-1.22505	2.83501	N(21)	Tyr 424
Exemestane	Arg 403	NE	-0.687485	2.83446	O(18)	Arg 403
		NH2	-0.322524	3.32084	O(18)	Arg 403
	Lys 473	N	-1.84649	3.19827	O(20)	Lys 473
Letrozole	Val 422	N	-2.5	3.09893	N(6)	Val 422
	Lys 440	N	-2.5	3.09986	N(2)	Lys 440
	Gln 428	NE2	-2.49168	3.10166	N(2)	Gln 428

Table 9 Properties of steric interaction between top 3 docking poses of DKC derivative and exemestane, anastrozole, and letrozole with PDB ID: 3S79

Molecule ID	Interacting amino acid	Interaction distance in Å	Strength	Interacting ligand atom	
DKC-1	His 475	3.30	0.01	C(23)	
		3.28	0.11	C(17)	
	Gln 367	3.28	0.10	C(9)	
	Lys 473	3.10	1.24	C(17)	
		2.84	2.81	O(6)	
	Tyr 366	3.17	0.78	O(13)	
	Met 68	3.19	0.67	O(22)	
	DKC-10	Arg 400	3.00	1.79	C(28)
			2.77	3.18	C(9)
			3.21	0.56	C(8)
2.21			0.77	O(21)	
Arg 79		2.49	4.92	C(26)	
Leu 479		3.29	0.04	C(13)	
Arg 403		3.14	0.99	C(28)	
		2.88	2.53	O(22)	
His 475		3.10	1.24	C(11)	
		2.92	2.30	C(29)	
DKC-20	Lys 473	3.22	0.47	N(48)	
		3.26	0.23	C(29)	
	Met 68	3.25	0.32	C(17)	
		3.28	0.15	O(51)	
	Trp 67	3.19	0.68	O(62)	
		3.23	0.44	C(60)	
	Ser 72	3.17	0.78	O(51)	
	Lys 230	2.26	6.32	C(22)	
		3.18	0.72	C(10)	
	DKC-21	Tyr 244	3.28	0.12	C(11)
3.06			1.43	C(40)	
Asp 222		2.28	6.19	C(35)	
		2.60	4.24	C(32)	
Gln 218		2.60	4.24	C(32)	
Phe 221		3.28	0.12	C(36)	
		3.19	0.64	C(32)	
Glu 483		3.28	0.11	C(28)	
		3.17	0.79	C(29)	
Pro 481		2.82	2.92	C(30)	
	3.30	0.03	C(31)		
His 480	3.08	1.32	C(30)		
	3.01	1.75	O(42)		
DKC-21	Gln 218	3.14	0.98	C(13)	
		Glu 483	3.03	1.62	O(17)

Table 9 (continued)

Molecule ID	Interacting amino acid	Interaction distance in Å	Strength	Interacting ligand atom	
DKC-1	Asp 222	3.24	0.36	C(8)	
		Ile 474	3.30	0.03	C(1)
	Lys 230	3.18	0.71	C(24)	
		2.52	4.74	C(32)	
	Gln 225	3.17	0.77	C(1)	
	Ala 226	3.24	0.34	O(33)	
		Met 68	2.99	1.87	C(37)
	Anastrozole	Met 68	3.18	0.72	O(36)
			Val 422	2.65	3.94
		Pro 429	3.24	0.35	C(1)
2.90			2.41	C(19)	
Exemestane		His 475	2.92	2.29	C(19)
		Lys 473	3.16	0.83	C(3)
Letrozole		Lys 473	3.15	0.89	C(10)
			Leu 479	3.28	0.14
		Phe 427	3.14	0.95	C(13)
			Met 444	2.74	3.41
	Phe 430	3.19	0.64	C(12)	
		Gln 428	2.63	4.09	C(7)

on $Er\alpha+$ (Fig. 7e). The results received through these interactions are very poor in terms of MolDock score, H-bonding, and steric interaction in comparison with DKC derivatives. On the other hand, exemestane, anastrozole, and, letrozole have been taken for study against p450 enzyme (Fig. 8e–g), since these medications block aromatase, but, here also inadequate MolDock score, hydrogen bonding, and steric interactions received. Therefore, it is possible to argue that DKC derivatives, might be superior therapeutic agents for treating breast cancer.

Furthermore, in the ADME/pharmacokinetics predictions profile, the foremost step of oral bioavailability of the drug can be determined by the drug aqueous solubility as well as intestinal permeability [56]. The results revealed that DKC-1 and its 3 derivatives have high gastrointestinal absorption, and then DKC-10 and DKC-21 possess P-glycoprotein, whereas DKC-1 and DKC-21 possess barrier to P-glycoprotein. Further, DKC-10, DKC-20, and DKC-21 exhibit the barrier towards the blood–brain barrier (BBB) except DKC-1 (Table 11). Despite this, one

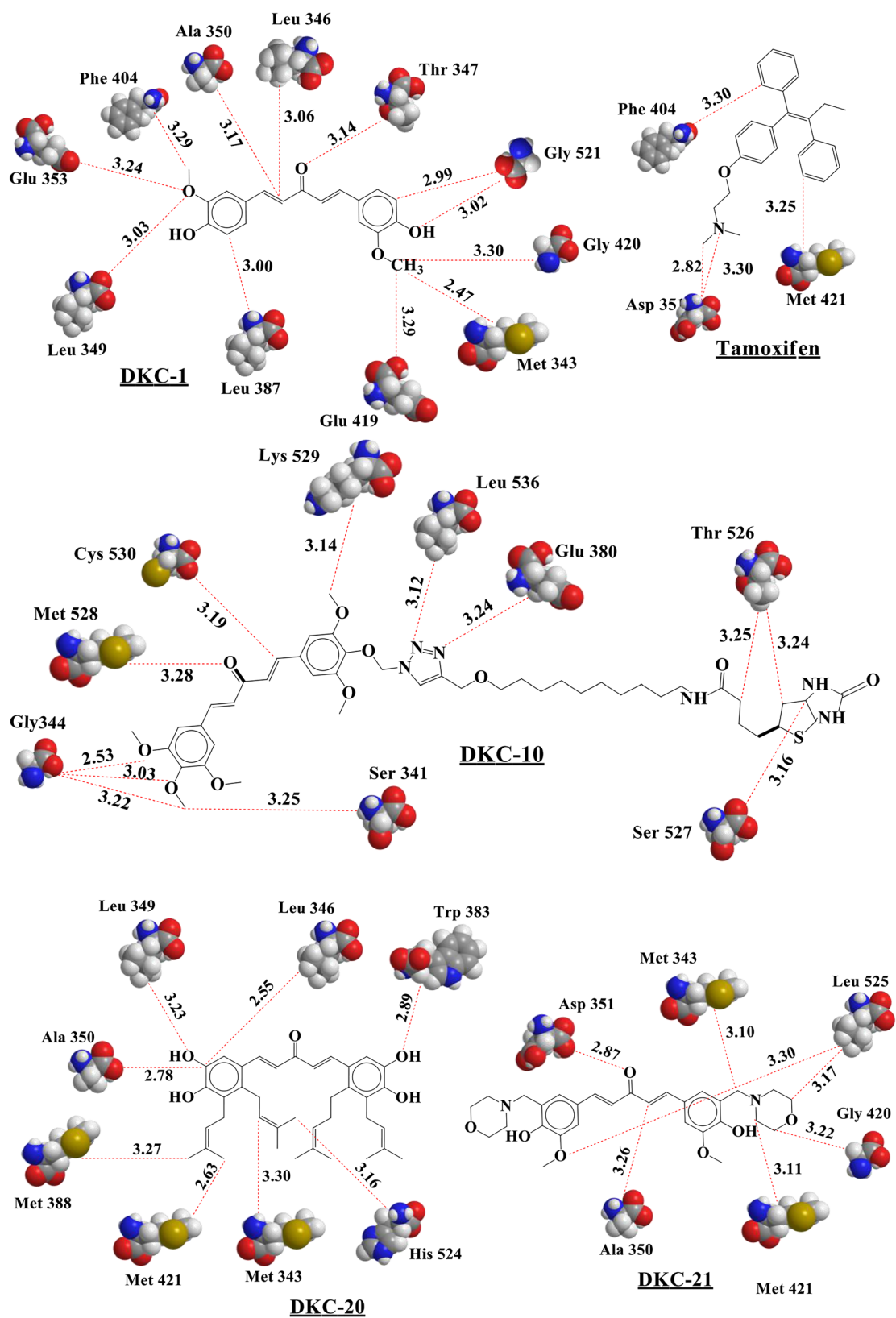


Fig. 9 Steric interactions (red-dotted bonds) displayed between ligands DKC-1, DKC-10, DKC-20, DKC-21, and tamoxifen with $Er\alpha+$ (PDB ID: 3ERT)

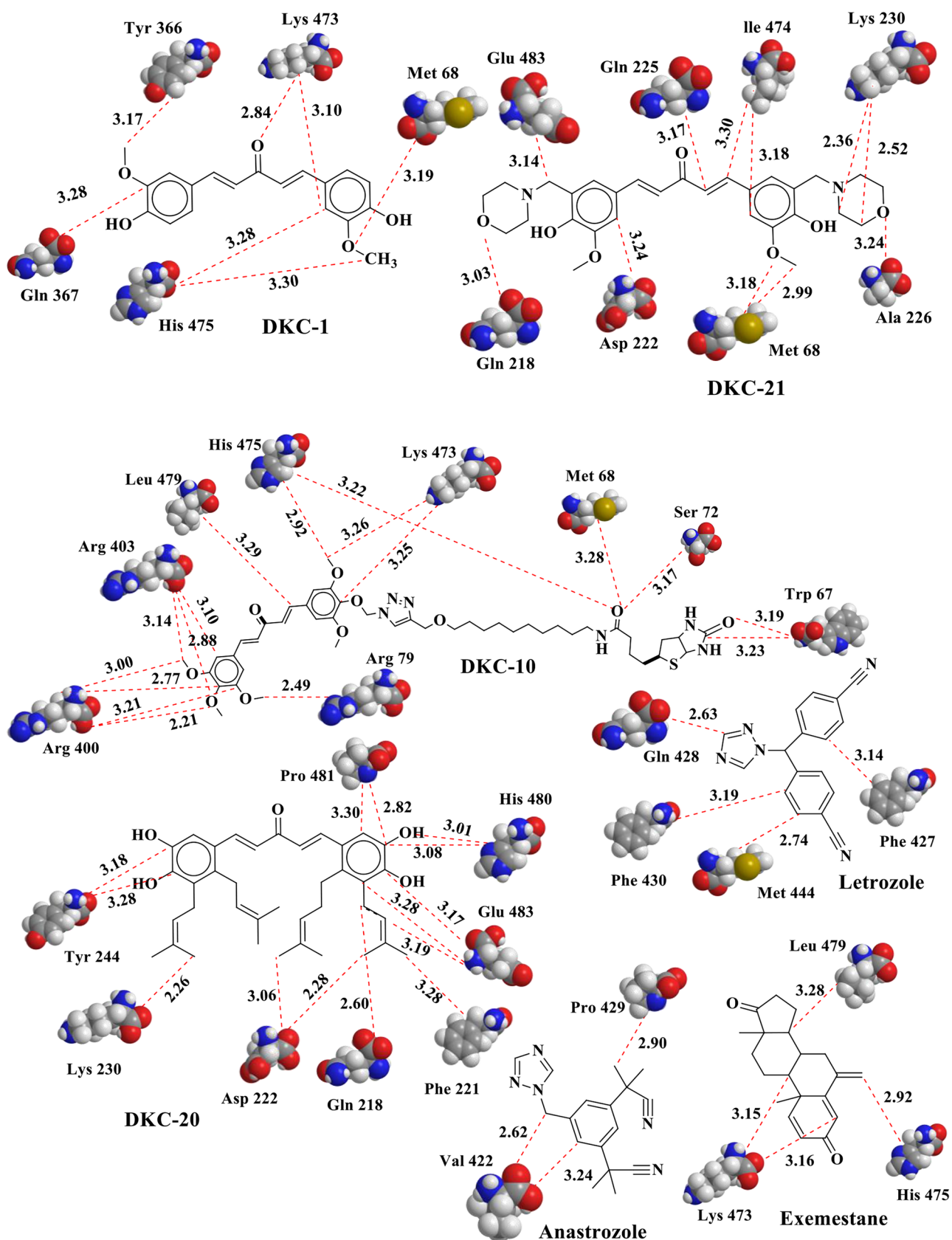


Fig. 10 Steric interactions (red-dotted bonds) displayed between ligands DKC-1, DKC-10, DKC-20, DKC-21, exemestane, anastrozole, and letrozole with aromatase (PDB ID: 3S79)

Table 10 Protein–ligand binding energies of known medicines and four DKC ligands were compared using MVD with two distinct PDB IDs

3ERT		3S79	
Ligand	Energy, kcal/mol or MolDock score	Existing drug	Energy, kcal/mol or score
DKC-1	-125.271	Tamoxifen	-131.909
DKC-10	-204.461		
DKC-20	-177.278		
DKC-21	-161.958		

Ligand	Energy, kcal/mol or MolDock score	Existing drugs	Energy, kcal/mol or MolDock score
DKC-1	-98.215	Anastrozole	-107.965
DKC-10	-201.613	Exemestane	-92.7947
DKC-20	-131.397	Letrozole	-108.904
DKC-21	-123.724		

Table 11 Parameters of ADME and drug-likeness of DKC-1 and its 3 derivatives

Ligand no.	nHA	nAHA	SA	GI	BBB	Pgp	MR	BS	MW (g/mol)	nHBA	nHBD	nRot	TPSA (Å)	iLOGP	WLOGP	nLV
DKC-1	24	12	2.76	High	Yes	No	92.99	0.55	326.34	5	2	6	75.99	3.10	3.19	0
DKC-10	62	17	7.70	High	No	Yes	247.92	0.17	879.07	10	3	30	207.92	7.18	5.81	1
DKC-20	36	12	4.12	High	No	No	154.84	0.17	620.37	5	0	12	53.99	6.09	8.00	1
DKC-21	38	12	3.98	High	No	Yes	152.61	0.55	524.61	9	2	10	100.93	4.68	1.79	1

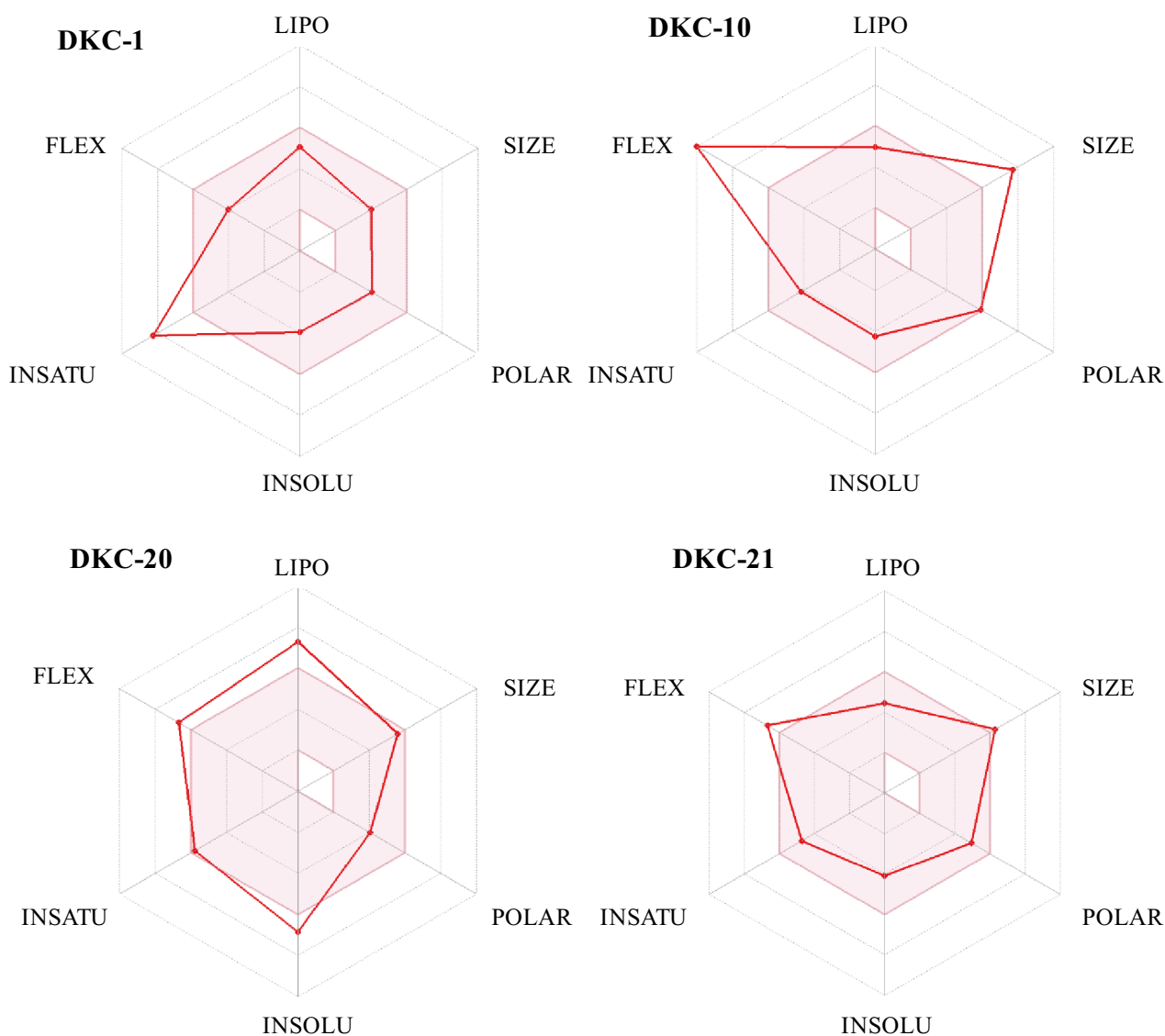


Fig. 11 Bioavailability radar of the lead molecules DKC derivatives

common violation has been observed in DKC-10, DKC-20, and DKC-21 due to molecular weight > 500 g/mol as per the Lipinski rule. Moreover, through SWISS ADME web server, boiled egg graph was also generated which illustrates absorption of the ligands in the gastrointestinal tract and brain. This type of graph is also known as the brain or intestinal estimated permeation predictive model or Egan egg graph [58]. The boiled egg graph of the four

DKC ligands has been shown in Fig. 11. Apart from this, Fig. 12 shows the bioavailability radar of the DKC-1 and its 3 derivatives based on six physicochemical properties such as lipophilicity, saturation, size, polarity, solubility, and flexibility [58]. Through radar images, it can be observed that DKC-1 and its 3 derivatives are expected to be orally bioavailable (less toxic and good absorption), less polarity, and low flexibility.

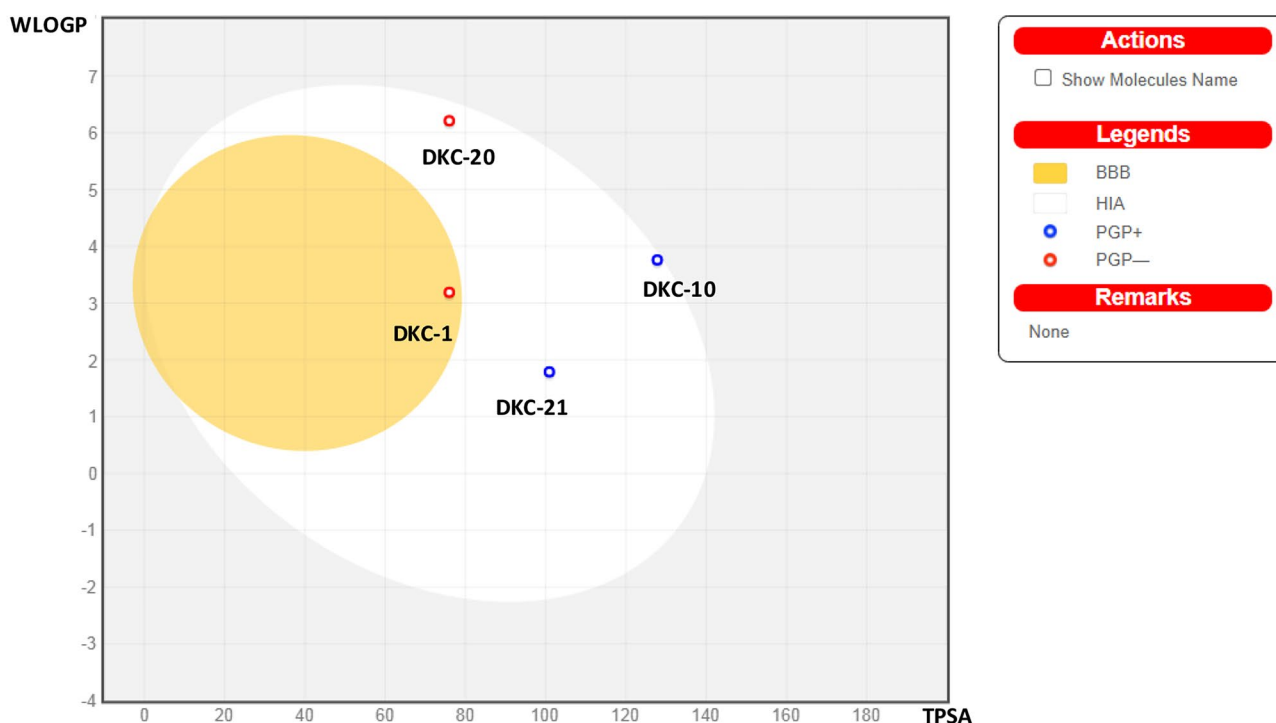


Fig. 12 Boiled egg graph of the most lead ligands DKC derivatives

Conclusion

Overall, it can be concluded that breast cancer in women is a serious global concern at the moment, as it ranks first on the list of cancers when compared to other malignancies. As a result, extensive research is being conducted to determine the most effective inhibitors for the treatment of breast cancer, particularly positive breast cancer. In this work, we discovered DKC derivatives' potential against breast cancer in both inhibitory pathways, such as an antagonist to $ER\alpha+$ and an inhibitor of the p450 cytochrome enzyme. The molecular docking study of 25 deketene curcumin derivatives have been conducted in this work against two proteins $ER\alpha+$ (PDB: 3ERT) and aromatase (PDB: 3S79), also carried out the comparative study with drugs that are already used to treat the breast cancer. From this study, three DKC derivatives DKC-10, DKC-20, and DKC-21 are discovered with the lowest binding affinity by interaction with $ER\alpha+$ and aromatase (-204.461 kcal/mol, -177.279 kcal/mol, -161.958 kcal/mol, and -201.613 , -131.397 , -123.724 , respectively). However, other parameters of these derivatives such as H-bonding and steric interactions are more favorable for the inhibition of $ER\alpha+$ (positive type of breast cancer host) in comparison with aromatase. In addition to this, docking study of existing drugs with breast cancer reveals poor outcomes in terms of MolDock score, H-bonding, and steric interactions in contrast to DKC

derivatives. Besides this, satisfactory results were received in the ADME/pharmacokinetics study of DKC derivatives. Therefore, it can be said that DKC-10, DKC-20, and DKC-21 are the leading candidate to treat a positive type of breast cancer. Apart from this, in the future, these candidates should be undergone the process of pre-clinical trials such as in vivo and in vitro studies against breast cancer.

Abbreviations AIs: Aromatase inhibitors; ADMET: Absorption, distribution, metabolism, excretion, and toxicity; $ER\alpha+$: Estrogen receptor-alpha positive; $ER+$: Estrogen receptor positive; $ER-$: Estrogen receptor negative; PR: Progesterone; HER2: Human epidermal growth factor receptor 2; EDBC: Estrogen-dependent breast cancer; ASD: Androstenedione; SERM: Selective estrogen receptor modulator; SERD: Selective estrogen down receptor; MVD: Molegro Virtual Docker; MVV: Molegro Virtual Viewer; DKC: Deketene curcumin; PDB: Protein Data Bank; PCOS: Polycystic ovary syndrome; WHO: World Health Organization

Supplementary information The online version contains supplementary material available at <https://doi.org/10.1007/s11224-021-01871-2>.

Acknowledgements The authors would like to thank the Swiss Institute of Bioinformatics for the SWISS ADME web server.

Author contribution All authors contributed to the study conception and design. Material preparation, data collection, and analysis were performed by Vraj Shah, Jaydip Bhaliya, and Gautam M. Patel. The first draft of the manuscript was written by Vraj Shah, and all authors commented on previous versions of the manuscript. All authors read and approved the final manuscript.

Declarations

Conflict of interest The authors declare no competing interests.

References

- Mansoori B, Mohammadi A, Gjerstorff MF, Shirjang S, Asadzadeh Z, Khaze V, Holmskov U, Kazemi T, Dulif PH, Baradaran B (2019) miR-142-3p is a tumor suppressor that inhibits estrogen receptor expression in ER-positive breast cancer. *J Cell Physiol* 234(9):16043–16053. <https://doi.org/10.1002/jcp.28263>
- Henriksen EL, Carlsen JF, Vejborg IM, Nielsen MB, Lauridsen CA (2019) The efficacy of using computer-aided detection (CAD) for detection of breast cancer in mammography screening: a systematic review. *Acta radiol* 60(1):13–18. <https://doi.org/10.1177/2F0284185118770917>
- Ferlay J, Soerjomataram I, Dikshit R, Eser S, Mathers C, Rebelo M, Parkin DM, Bray FD (2015) Cancer incidence and mortality worldwide: sources, methods and major patterns in GLOBOCAN 2012. *Int J Cancer* 136(5):359–386. <https://doi.org/10.1002/ijc.29210>
- World Health Organisation (WHO) (2021) Databank. Health statistics and information systems Geneva, Switzerland: WHO. <https://www.who.int/cancer/prevention/diagnosis-screening/breast-cancer/en/> Accessed 20 Aug 2021. World Health Organisation (WHO), Breast Cancer. <https://www.who.int/news-room/fact-sheets/detail/breast-cancer>. Accessed 20 Aug 2021
- Awasthi M, Singh S, Pandey VP, Dwivedi UN (2015) Molecular docking and 3D-QSAR-based virtual screening of flavonoids as potential aromatase inhibitors against estrogen-dependent breast cancer. *J Biomol Struct Dyn* 33(4):804–819. <https://doi.org/10.1080/07391102.2014.912152>
- Lim S, Janzer A, Becker A, Zimmer A, Schüle R, Buettner R, Kirfel J (2010) Lysine-specific demethylase 1 (LSD1) is highly expressed in ER-negative breast cancers and a biomarker predicting aggressive biology. *Carcinogenesis* 31(3):512–520. <https://doi.org/10.1093/carcin/bgp324>
- Gil EMC (2014) Targeting the PI3K/AKT/mTOR pathway in estrogen receptor-positive breast cancer. *Cancer Treat Rev* 40(7):862–871. <https://doi.org/10.1016/j.ctrv.2014.03.004>
- Anderson WF, Chatterjee N, Ershler WB, Brawley OW (2002) Estrogen receptor breast cancer phenotypes in the Surveillance, Epidemiology, and End Results database. *Breast Cancer Res Treat* 76(1):27–36. <https://doi.org/10.1023/A:1020299707510>
- Cleator SJ, Ahamed E, Coombes RC, Palmieri C (2009) A 2009 update on the treatment of patients with hormone receptor—positive breast cancer. *Clin Breast Cancer* 9:S6–S17. <https://doi.org/10.3816/CBC.2009.s.001>
- Davies E, Hiscox S (2011) New therapeutic approaches in breast cancer. *Maturitas* 68(2):121–128. <https://doi.org/10.1016/j.maturitas.2010.10.012>
- Lee HR, Kim TH, Choi KC (2012) Functions and physiological roles of two types of estrogen receptors, ER α and ER β , identified by estrogen receptor knockout mouse. *Lab Anim Res* 28(2):71. <https://doi.org/10.5625/lar.2012.28.2.71>
- Hong Y, Li H, Yuan YC, Chen S (2009) Molecular characterization of aromatase. *Ann N Y Acad Sci* 1155:112. <https://doi.org/10.1111/2Fj.1749-6632.2009.03703.x>
- Chan HJ, Petrossian K, Chen S (2016) Structural and functional characterization of aromatase, estrogen receptor, and their genes in endocrine-responsive and-resistant breast cancer cells. *J Steroid Biochem Mol Biol* 161:73–83. <https://doi.org/10.1016/j.jsbmb.2015.07.018>
- Almeida CF, Teixeira N, Oliveira A, Augusto TV, Correia-da-Silva G, Ramos MJ, Fernandes PA, Amaral C (2021) Discovery of a multi-target compound for estrogen receptor-positive (ER+) breast cancer: involvement of aromatase and ERs. *Biochimie* 181:65–76. <https://doi.org/10.1016/j.biochi.2020.11.023>
- Miller WR (2003) Aromatase inhibitors: mechanism of action and role in the treatment of breast cancer. *Semin Oncol* 30:3–11. [https://doi.org/10.1016/S0093-7754\(03\)00302-6](https://doi.org/10.1016/S0093-7754(03)00302-6)
- Ballinger TJ, Meier JB, Jansen VM (2018) Current landscape of targeted therapies for hormone-receptor positive, HER2 negative metastatic breast cancer. *Front Oncol* 8:308. <https://doi.org/10.3389/fonc.2018.00308>
- Fontham ET, Thun MJ, Ward E, Balch AJ, Delancey JO, Samet JM (2009) American Cancer Society perspectives on environmental factors and cancer. *CA Cancer J Clin* 59(6):343–351. <https://doi.org/10.3322/caac.20041>
- Wong C, Chen S (2012) The development, application and limitations of breast cancer cell lines to study tamoxifen and aromatase inhibitor resistance. *J Steroid Biochem Mol Biol* 131(3–5):83–92. <https://doi.org/10.1016/j.jsbmb.2011.12.005>
- Dutta U, Pant K (2008) Aromatase inhibitors: past, present and future in breast cancer therapy. *Medical Oncology* 25(2):113–124. <https://doi.org/10.1007/s12032-007-9019-x>
- Thürlimann B, Hess D, Köberle D, Senn I, Ballabeni P, Pagani O, Perey L, Aebi S, Rochlitz C, Goldhirsch A (2004) Anastrozole ('Arimidex') versus tamoxifen as first-line therapy in postmenopausal women with advanced breast cancer: results of the double-blind cross-over SAKK trial 21/95—a sub-study of the TARGET (Tamoxifen or 'Arimidex' Randomized Group Efficacy and Tolerability) trial. *Breast Cancer Res Treat* 85(3):247–254. <https://doi.org/10.1023/B:BREA.0000025420.78346.f9>
- Setti A, Venugopal Rao V, Priyamvada Devi A, Pawar SC, Naresh B, Kalyan CS (2012) Impact of Aromatase protein variants and drug interactions in breast cancer: a molecular docking approach. *J Recept Signal Transduct* 32(4):225–229. <https://doi.org/10.3109/10799893.2012.693088>
- Cancer Center Hormone therapy for Breast Cancer (2021) <https://www.webmd.com/breast-cancer/guide/breast-cancer-hormone-therapy-choices>. Accessed 15 Aug 2021
- Breast cancer now, Side effect of letrozole (2021) <https://breastcancernow.org/information-support/facing-breast-cancer/going-through-breast-cancer-treatment/side-effects-letrozole-femara>. Accessed 15 Aug 2021
- Verma SK, Ratre P, Jain AK, Liang C, Gupta GD, Thareja S (2021) De novo designing, assessment of target affinity and binding interactions against aromatase: discovery of novel leads as anti-breast cancer agents. *Struct Chem* 32(2):847–858. <https://doi.org/10.1007/s11224-020-01673-y>
- Tilak Vijay J, Babu KV, Uma A (2019) Virtual screening of novel compounds as potential ER-alpha inhibitors. *Bioinformation* 15(5):321. <https://doi.org/10.6026/2F97320630015321>
- Breast cancer now, Side effect of anastrozole (2021) <https://breastcancernow.org/information-support/facing-breast-cancer/going-through-breast-cancer-treatment/side-effects-anastrozole-arimidex>. Accessed 16 Aug 2021
- Banjare L, Verma SK, Jain AK, Thareja S (2020) Design and pharmacophoric identification of flavonoid scaffold-based aromatase inhibitors. *J Heterocycl Chem* 57(9):3483–3492. <https://doi.org/10.1002/jhet.4068>
- Rahma M, Hossain S (2015) In silico computational prediction of anti-breast cancer effect of abruquinones from *Abrus precatorius* L. *BRC* 1(1):22–27
- Bhaliya J, Shah V (2020) Identification of potent COVID-19 main protease (Mpro) inhibitors from curcumin analogues by molecular docking analysis. *Int J Adv Res Ideas Innov Technol* 6(2):664–672

30. Anbarasu K, Jayanthi S (2018) Identification of curcumin derivatives as human LMTK3 inhibitors for breast cancer: a docking, dynamics, and MM/PBSA approach. *3 Biotech* 8(5):1–12. <https://doi.org/10.1007/s13205-018-1239-6>
31. Cen L, Hutzen B, Ball S, DeAngelis S, Chen CL, Fuchs JR, Li C, Li PK, Lin J (2009) New structural analogues of curcumin exhibit potent growth suppressive activity in human colorectal carcinoma cells. *BMC cancer* 9(1):1–8. <https://doi.org/10.1186/1471-2407-9-99>
32. Liang G, Shao L, Wang Y, Zhao C, Chu Y, Xiao J, Zhao Y, Li X, Yang S (2009) Exploration and synthesis of curcumin analogues with improved structural stability both in vitro and in vivo as cytotoxic agents. *Bioorg Med Chem* 17(6):2623–2631. <https://doi.org/10.1016/j.bmc.2008.10.044>
33. Suarez JA, Rando DG, Santos RP, Gonçalves CP, Ferreira E, de Carvalho JE, Kohn L, Maria DA, Faião-Flores F, Michalik D, Marcucci MC (2010) New antitumoral agents I: in vitro anticancer activity and in vivo acute toxicity of synthetic 1, 5-bis (4-hydroxy-3-methoxyphenyl)-1, 4-pentadien-3-one and derivatives. *Bioorg Med Chem* 18(17):6275–6281. <https://doi.org/10.1016/j.bmc.2010.07.026>
34. Chou KC (2004) Structural bioinformatics and its impact to biomedical science. *Curr Med Chem* 11(16):2105–2134. <https://doi.org/10.2174/0929867043364667>
35. Schneider G, Böhm HJ (2002) Virtual screening and fast automated docking methods. *Drug Discov* 7:64–70. [https://doi.org/10.1016/S1359-6446\(02\)00004-1](https://doi.org/10.1016/S1359-6446(02)00004-1)
36. Zekri A, Harkati D, Kenouche S, Saleh BA (2020) QSAR modeling, docking, ADME and reactivity of indazole derivatives as antagonists of estrogen receptor alpha (ER- α) positive in breast cancer. *J Mol Struct* 1217:128442. <https://doi.org/10.1016/j.molstruc.2020.128442>
37. Abdellah AM, Sliem MA, Bakr M, Amin RM (2018) Green synthesis and biological activity of silver–curcumin nanoconjugates. *Future Med Chem* 10(22):2577–2588. <https://doi.org/10.4155/fmc-2018-0152>
38. Shiau AK, Barstad D, Loria PM, Cheng L, Kushner PJ, Agard DA, Greene GL (1998) The structural basis of estrogen receptor/coactivator recognition and the antagonism of this interaction by tamoxifen. *Cell* 95(7):927–937. [https://doi.org/10.1016/S0092-8674\(00\)81717-1](https://doi.org/10.1016/S0092-8674(00)81717-1)
39. Ghosh D, Lo J, Morton D, Valette D, Xi J, Griswold J, Hubbell S, Egbuta C, Jiang W, An J, Davies HM (2012) Novel aromatase inhibitors by structure-guided design. *J Med Chem* 55(19):8464–8476. <https://doi.org/10.1021/jm300930n>
40. Shah VR, Bhaliya JD, Patel GM (2021) In silico approach: docking study of oxindole derivatives against the main protease of COVID-19 and its comparison with existing therapeutic agents. *J Basic Clin Physiol Pharmacol* 32(3):197–214. <https://doi.org/10.1515/jbcpp-2020-0262>
41. Dahmke IN, Boettcher SP, Groh M, Mahlke U (2014) Cooking enhances curcumin anti-carcinogenic activity through pyrolytic formation of deketene curcumin. *Food Chem* 151:514–519. <https://doi.org/10.1016/j.foodchem.2013.11.102>
42. Sardjiman SS, Reksahadiprodjo MS, Hakim L, Van der Goot H, Timmerman H (1997) 1, 5-Diphenyl-1, 4-pentadiene-3-ones and cyclic analogues as antioxidant agents. Synthesis and structure-activity relationship. *Eur J Med Chem* 32(7–8):625–630. [https://doi.org/10.1016/S0223-5234\(97\)83288-6](https://doi.org/10.1016/S0223-5234(97)83288-6)
43. Fuchs JR, Pandit B, Bhasin D, Etter JP, Regan N, Abdelhamid D, Li C, Lin J, Li PK (2009) Structure–activity relationship studies of curcumin analogues. *Bioorganic Med Chem Lett* 19(7):2065–2069. <https://doi.org/10.1016/j.bmc.2009.01.104>
44. Kohyama A, Yamakoshi H, Hongo S, Kanoh N, Shibata H, Iwabuchi Y (2015) Structure-activity relationships of the antitumor C5-curcuminoid GO-Y030. *Molecules* 20(8):15374–15391. <https://doi.org/10.3390/molecules200815374>
45. Artico M, Di Santo R, Costi R, Novellino E, Greco G, Massa S, Tramontano E, Marongiu ME, De Montis A, La Colla P (1998) Geometrically and conformationally restrained cinnamoyl compounds as inhibitors of HIV-1 integrase: synthesis, biological evaluation, and molecular modeling. *J Med Chem* 41(21):3948–3960. <https://doi.org/10.1021/jm9707232>
46. Suárez JA, Peseke K, Kordian M, Carvalho JE, Kohn LK, Antônio MA, Brunhari H (2008) Method for the preparation of 1, 5-bis (4-hydroxy-3-methoxy-phenyl)-penta-1, 4-dien-3-one and derivatives with antitumoral properties, U.S. Patent No. 7,432,401. Washington, DC: U.S. Patent and Trademark Office
47. Yerdelen KO, Gul HI, Sakagami H, Umemura N (2015) Synthesis and biological evaluation of 1, 5-bis (4-hydroxy-3-methoxyphenyl) penta-1, 4-dien-3-one and its aminomethyl derivatives. *J Enzyme Inhib Med Chem* 30(3):383–388. <https://doi.org/10.3109/14756366.2014.940934>
48. Thomsen R, Christensen MH (2006) MolDock: a new technique for high-accuracy molecular docking. *J Med Chem* 49(11):3315–3321. <https://doi.org/10.1021/jm051197e>
49. Naeem S, Hylands P, Barlow D (2013) Docking studies of chlorogenic acid against aldose reductase by using molgro virtual docker software. *J Appl Pharm Sci* 3(1):13–20. <https://doi.org/10.7324/JAPS.2013.30104>
50. Verma SK, Thareja S (2017) Structure based comprehensive modelling, spatial fingerprints mapping and ADME screening of curcumin analogues as novel ALR2 inhibitors. *Plos One* 12(4):e0175318. <https://doi.org/10.1371/journal.pone.0175318>
51. Gehlhaar DK, Bouzida D, Rejto PA (1998) In Porto VW, Saravanan N, Waagen D, Eiben AE (eds) Fully automated and rapid flexible docking of inhibitors covalently bound to serine proteases, (pp. 449–461) Springer, Berlin, Heidelberg. <https://doi.org/10.1007/BFb0040797>
52. Yang JM, Chen CC (2004) GEMDOCK: a generic evolutionary method for molecular docking. *Proteins* 55(2):288–304. <https://doi.org/10.1002/prot.20035>
53. Umar AB, Uzairu A, Shallangwa GA, Uba S (2020) Design of potential anti-melanoma agents against SK-MEL-5 cell line using QSAR modeling and molecular docking methods. *SN Appl Sci* 2(5):1–18. <https://doi.org/10.1007/s42452-020-2620-8>
54. Attique SA, Hassan M, Usman M, Atif RM, Mahboob S, Al-Ghanim KA, Bilal M, Nawaz MZ (2019) A molecular docking approach to evaluate the pharmacological properties of natural and synthetic treatment candidates for use against hypertension. *Int J Environ Res Public Health* 16(6):923. <https://doi.org/10.3390/ijerph16060923>
55. Swiss Institute of Bioinformatics (2021) <http://www.swissadme.ch/>. Accessed 20 Aug 2021
56. Daina A, Michielin O, Zoete V (2017) SwissADME: a free web tool to evaluate pharmacokinetics, drug-likeness and medicinal chemistry friendliness of small molecules. *Sci Rep* 7(1):1–13. <https://doi.org/10.1038/srep42717>
57. Abdullahi M, Adeniji SE (2020) In-silico molecular docking and ADME/pharmacokinetic prediction studies of some novel carboxamide derivatives as anti-tubercular agents. *Chem Afr* 3(4):989–1000. <https://doi.org/10.1007/s42250-020-00162-3>
58. Daina A, Zoete V (2016) A boiled-egg to predict gastrointestinal absorption and brain penetration of small molecules. *Chem Med Chem* 11(11):1117–1121. <https://doi.org/10.1002/Fcmcdc.201600182>

Publisher's Note Springer Nature remains neutral with regard to jurisdictional claims in published maps and institutional affiliations.